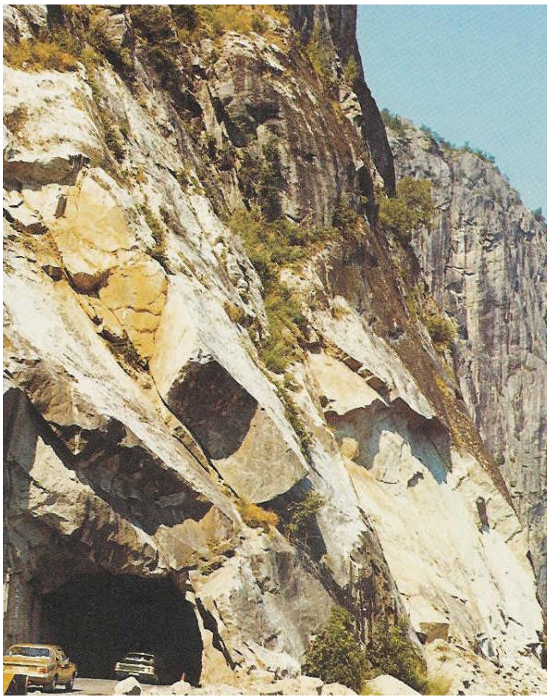

# Q-SYSTEM - AN ILLUSTRATED GUIDE FOLLOWING FORTY YEARS IN TUNNELLING


**N. Barton and E. Grimstad 2014**


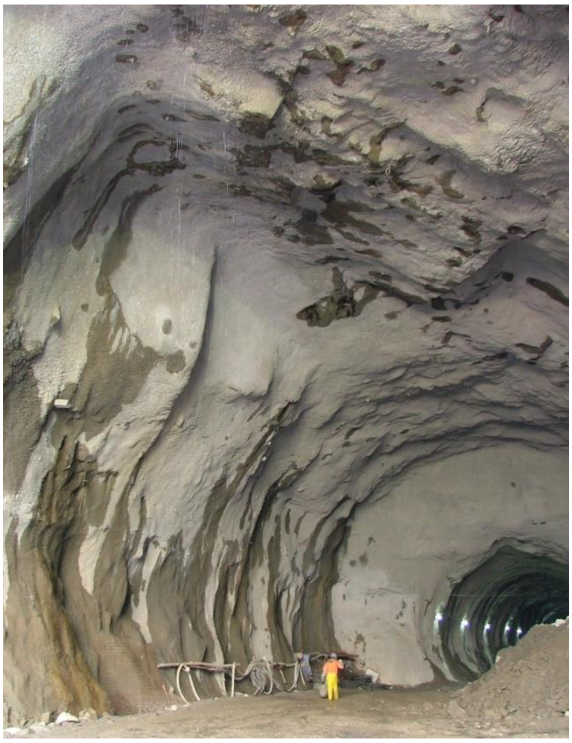


www.nickbarton.com

# Q-System - An Illustrated Guide following Forty years in Tunnelling.

Nick Barton [1] and Eystein Grimstad [2]

[1] Nick Barton & Associates, Høvik, Norway, nickrbarton@hotmail.com

[2] Geolog Eystein Grimstad, Oslo, Norway, eystein.grimstad@vikenfiber.no

ABSTRACT

This paper provides a well-illustrated guide to the workings of the Q-system, with many examples demonstrating its use. Not only rock exposure logging, but also core-logging, and tunnel-logging are illustrated with quantified examples. The Q-system was developed 40 years ago for describing rock mass quality in a quantitative way, using six important parameters and ratings of quality. These were first related to structural geology, in particular the number of joint sets, their roughness, whether there was clay-filling, followed by the effects of water and the stress/strength ratio. A logarithmic-like scale from about 0.001 to 1000 was the result. All the ratings of the key parameters are given in this guide, and include footnotes and a field-logging sheet and examples of its use. Linked to the Q-value and the span or height of the excavation in rock, and also reflecting the final purpose of the excavation, is an updated chart of recommended support and reinforcement for the arch and walls of underground excavations. Both tunnels and caverns are catered for, from roughly 3m to 60m span. Some 20 years ago the S(mr) support was updated by the same authors, replacing mesh reinforced shotcrete with fiber reinforced sprayed concrete or S(fr). The recommended PVC-sleeved (CT) bolts were more resistant to corrosion. The Q-system has always reflected single-shell B+S(fr) concepts of permanent support, as encompassed in the Norwegian Method of Tunnelling (NMT). During the 40 years of its use the Q-value has been shown to have empirical relationships to seismic velocity, deformation modulus, and tunnel or cavern deformation. It can also be used for helping to quantify the benefits of high-pressure pre-injection, and to estimate permeability. In addition, the Q-value has been extended for use in TBM prognosis, and a brief graphic review of this is given.

**Key words:** rock mass, classification, tunnels, drill-core, rock support, seismic velocity.

## Introduction

Norway is a country with a small population, yet 3,500 km of hydro-power related tunneling, about 180 underground power houses, and some 1,500 km of road and rail tunnels. This has meant that *economic* tunnels, power-houses and also storage caverns, have always been needed, especially prior to the development of North Sea petroleum resources. The Q-system development in 1973 always reflected this, and single-shell tunnel support and reinforcement, meaning shotcrete and rock bolts as final support has been the norm, both before and since Q-system development. The first 200-plus case records from which Q was developed were 60% from Scandinavia, and already represented *fifty different rock types*, which is perhaps surprising for those who may focus on the quite frequent pre-Cambrian granites and gneisses. Norwegian and Swedish hydro power projects dominated these early cases, giving a wide range of excavation sizes and uses (i.e. access tunnels, headrace tunnels, powerhouses). An update of the Q-system support methods, presented by Grimstad and Barton (1993), was based on 1,050 new case records collected between 1986 and 1993. These were deliberately chosen to be independent of Q-system application. They were mostly developed from road tunnel projects, where higher levels of support were generally used. This update specifically replaced S(mr) with S(fr), meaning the replacement of steel mesh with steel fibre-reinforced shotcrete. In 2002, approximately 800 more case records were added, giving further independent measures of S(fr) thickness and bolt spacing. The Q-value had been logged, but was not used in many cases. Some inconsistent results can be noted, including three collapses where Q-recommendations were not used. (Appendix A4). Users of the Q-system should note that an unchecked version of Q with several errors has recently been promoted by NGI despite the present authors' lack of participation or approval. These younger authors were (clearly) not present during original development of Q, nor participated in its case record based update in 1993.

## How and why Q was developed

A question from the Norwegian State Power Board (Statkraft) which was passed to the first author at NGI in 1973, was the following: 'Why are Norwegian powerhouses showing such a wide range of deformations'? A lack of quantitative methods for describing rock quality in 1973, besides Deere's RQD from 1964, and the need to consider excavation dimensions, depth and possible stress levels, together with the different support measures used at that time, meant that a new and integrated method was needed. After 6 months of extensive case record study, using a successively updated list of rock mass parameters and constantly updated ratings, the Statkraft question could finally be answered. This 6 months delay saw the development of the Q-system (Barton, Lien and Lunde 1974), which has eventually become one of the main rock mass classification methods used throughout the world of mining and civil engineering. It is often used alongside RQD and RMR (Bieniawski 1989), both of which were developed before Q. Both RMR and Q have made use of RQD, and in the case of Q, the RQD % is used directly, unless it is < 10%. (The minimum used is 10%).

## Classification method briefly described

Trial and error using two, three, four and finally six parameters, with successive adjustment of ratings to get the best fit between rock quality, excavation dimensions, and support quantities, resulted in one of the simplest equations regularly used in rock engineering.

$$Q = \frac{RQD}{J_n} \times \frac{J_r}{J_a} \times \frac{J_w}{SRF} \tag{1}$$

Due to the need for the rock mass classification to fit the case records, the ratings and format of the Q-equation eventually resulted in something resembling a log-scale, with Q ranging from approximately 0.001 to 1000, from the worst (faulted, squeezing, water-bearing) conditions, to the best (massive dry) conditions. The formal definitions and ratings of the six parameters are tabulated in Appendix A1. It should be noted that the three pairs of parameters *RQD/number of joint sets, joint roughness/joint alteration-filling, water/stress-strength,* resemble, in very approximate terms: block size, inter-block shear strength and active stress.

*Table 1 A short summary of the Q-system parameters and the case record back-ground.*

| **Q-parameter definitions** | **Q case-record back-ground** |
|---|---|
| **RQD** is the % of *competent* drill-core sticks > 100 mm in length *in a selected domain*. (In tunnel mapping imagine cores or scan-lines). | The initial data base in 1973 was 212 cases of single-shell tunnels and caverns, for hydropower, road, rail, storage, sewage. |
| **Jn** = the rating for the number of joint sets (9 for 3 sets, 4 for 2 sets etc.) *in the same domain.* | About 60% of the initial cases were from Scandinavia and about 40% were from Europe, USA, etc. |
| **Jr** = the rating for the roughness of the *least favourable* of these joint sets or filled discontinuities, *in the same domain.* | About 50% of the initial cases were from hydropower projects in Norway and Sweden. |
| **Ja** = the rating for the degree of alteration or clay filling of the *least favourable* of these joint sets or filled discontinuities, *in the same domain.* | Fifty rock types were initially represented. The majority were igneous and metamorphic rocks, with a smaller number of weak sedimentary rocks. |
| **Jw** = the rating for the water inflow and pressure effects, which may cause outwash of discontinuity infillings, *in the same domain.* | Numerous shear zones and faults containing clay, and numerous cases with clay-coated and clay-filled joints were included. |
| **SRF** = the rating for faulting, for strength/stress ratios in hard massive rocks, for *squeezing* or for swelling *in soft rock – in the same domain.* | Numerous cases of weathered conditions were also included, with all Q-parameters adversely affected. |
| (Note: in the 1993 update, three new high-SRF classes related to the observed effects of high stress and extreme support needs were added, specifically for the case of 'spalling' and 'bursting' in initially *massive rock*). See Appendix A1, Table 6b, L, M and N. Stress-induced fracturing: $\sigma_{\theta(max)} > 0.4\sigma_c$ (However in deep mines with significant numbers of joint sets one should use the original lower SRF values from 1974). | In 1993 another 1050 case records were added, mostly from road tunnels. S(mr) was replaced by S(fr) – fiber reinforced shotcrete. S(mr) for tunnel support was totally replaced by S(fr) by 1983. These updates provided case records in which the Q-recommendations were not used, ensuring 'independence'. In 2002, approximately 800 more cases of S(fr), RRS and bolt spacing for permanent support were added. The scatter seen in non-Q practice is sometimes wide and includes cases of cave in. See Appendix A4. There are now approximately 2,060 tunnelling/cavern cases in total, which lie behind the Q-support-and-reinforcement recommendations for tunnelling. |

The Q-system is designed to assist in feasibility studies, and to be actively used in detailed site characterization when mapping exposures, interpreting seismic velocities and logging drill-core. It is also used systematically once tunneling begins, since the mapped *rock class* following each blast can be a basis for selecting tunnel reinforcement (bolting) and support (fiber-reinforced shotcrete). Finite element modelling does not answer 'day-to-day (blast-by-blast) questions', so empiricism that works due to its track record is obviously essential. In the following sections we will give photographic examples of core logging, surface-exposure logging, and tunnel logging, so that potential users can get some feel for the method. The Q-system needs to be used by engineering geologists with some reliable training and experience behind them. The initial assessment naturally involves an evaluation of the degree of jointing, the number of joint sets: i.e. the general degree of fracturing and block-size, followed by an assessment of the most adverse Jr/Ja combination, taking into account favourable and unfavourable orientations. What is causing most over-break (e.g. Figure 1), and what would happen with no reinforcement or support? Experience is also essential in the determination of the necessary SRF category. Evaluation of this parameter involves knowing the depth or likely stress level in relation to the probable strength of the rock. The degree of stress-induced fracturing, if already occurring, or the amount of shearing and clay that is present in the case of fault zones, will each give clues to the appropriate value of SRF. Water inflow is also assessed, with or without the availability of Lugeon or permeability test results in the early stages of logging, and when local measurements are not available.

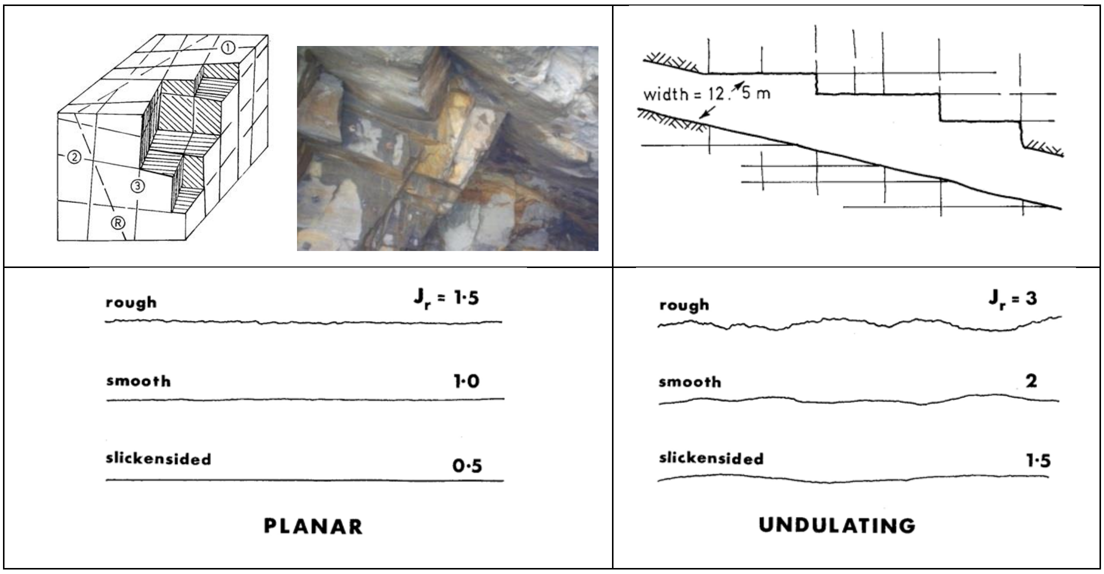


*Figure 1 Some graphic illustrations of the workings of the Q-parameters, using number of joint sets (Jn) and roughness (Jr). Sufficient numbers of joint sets may or may not cause over-break. When Jn/Jr ≥ 6, over-break becomes extremely likely, even with careful blasting. High Ja obviously assists here.*

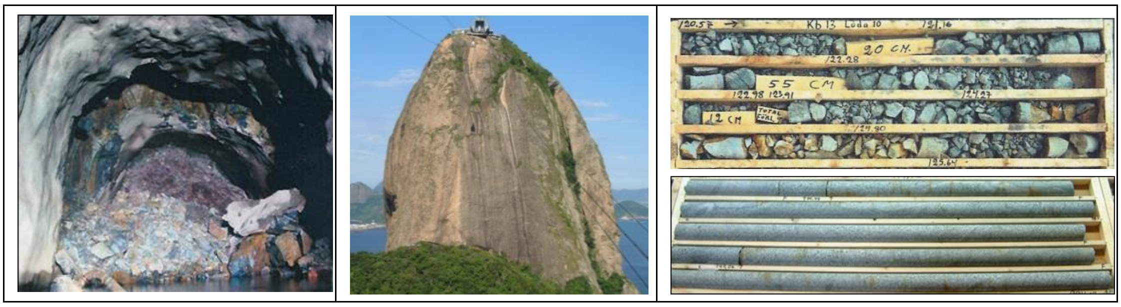

*Figure 2 Contrasting worst (Q ≈ 0.001) and best (Q ≈ 1000) rock mass qualities. The logarithmic appearance of the Q-value scale, stretching over six orders of magnitude, has proved to be a great advantage, and results in simple empirical equations for relating to velocity, modulus, and deformation. The large numerical range appears realistic when considering shear strength and modulus variation.*

## Examples of core-logging with Q

In projects where there are poor exposures due to weathering, the first sight of the rock may be via drill-core. It is strongly advised that a significant number, perhaps most of the bore holes, should be deviated from vertical, because of the frequency of sub-vertical structure which is poorly sampled by vertical holes. In a recent rail tunnel in Norway, all five boreholes were strongly deviated, thereby sampling folded and steeply tilted inter-bedding much more effectively. Vertical holes may give false higher quality, and unrealistically low permeabilities.

| | |
|---|---|
|  | 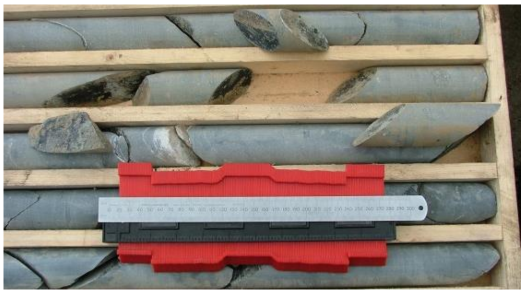 |
| Deeply weathered granite. Few pieces of this core box qualify for RQD assessment: i.e. 0, 20, 0, & 0 %. Change RQD of <10% to 10% when calculating Q. | Shale inter-bedded with limestone. Note recording of Jr = 1 and 1.5, therefore low roughness JRC. $Q_{range}$ = (30-50)/9 x (0.5-1)/(3-4)x0.66/1≈ 0.8-0.9. |
|  |  |
| Good quality granite sampled in a deviated hole. $Q_{range}$ = (65-100)/(6-9) x (1-1.5)/1 x 0.66/1 ≈ 5 – 25 Note that RQD continues its function when core pieces are > 10cm in length. RQD also indicates anisotropy. | Partly altered joints in tuff. When logging core close to tunnel depth (175m), the degree of joint connectivity gives clue to Jw prior to Lugeon tests. $Q_{range}$ = (10-25)/(12-15)x1.5/(2-4)x(0.5-0.66)/2.5≈0.1-0.3. |
|  |  |
| A weakness zone with swelling clay from the Finnfast sub-sea tunnel site investigation in Norway. Core-recovery from a bore hole drilled in a tunnel face. $Q_{range}$ ≈ 10/(15-20) x 1/(13-16)x(1.0-)/2.5 ≈ 0.01- 0.02. | Crushed zone in black shale from the Rogfast sub-sea tunnel site investigation. Seabed-to-borehole seismic tomography borehole. $Q_{range}$ ≈ (10-30)/(15-20)x(1-2)/(6-8)x(1.0-0.5)/2.5≈0.01-0.3. |

*Figure 3 Six contrasting core boxes from road and rail tunnel projects in Norway and Hong Kong. In both countries use of the Q-system for core logging and tunnel logging is required by the authorities. Concerning the two most challenging cases: the weakness zone in the Finnfast tunnel was quite dry both during core drilling and after excavation. There was little water in the drill hole at Rogfast.*

## Additional advice concerning core logging

Since drill cores are often missing where the rock quality is very poor due to poor recovery (e.g. see the plastic containers in Figure 3.1), the rock mass lack-of-quality has to be assessed by other methods, such as seismic velocity or resistivity. Where cores do exist, and there is good recovery, the first four of the Q-parameters may be evaluated with a relatively high degree of accuracy. However, special attention should be addressed to the following:

- Evaluation of the large and medium scale roughness parameter Jr may be difficult when joints are intersecting the borehole at an obtuse angle, due to short samples.
- As water is generally used during drilling, mineral fillings like softer clay minerals may be washed out, making it difficult to evaluate Ja in some cases.
- Joints sub-parallel to the borehole will be under-represented, and will give too high RQD-values and too low Jn-values. So both Q and permeability will be affected.
- RQD is often calculated for every meter. However Jn must usually be estimated for sections of several metres, by observing the core boxes from above and below.

- Water loss or Lugeon tests are often carried out during core drilling, and can form the basis for evaluation of the Jw-value. Since grouting often reduces the permeability, and tends to improve many Q-parameters, there will be an increase in the estimated Q-value in case of logging grouted sections of the rock mass.
- An estimation of SRF in massive rock can be made based on the height of overburden, or the height/steepness of an eventual mountain side. If stress measurements are carried out in boreholes, or experiences from nearby construction sites are available, these should be used so that the probable stress magnitude can be compared with an estimate or measurement of the uniaxial strength of the rock. (Core-disking and subsequent stress-induced fracturing around the tunnel each give clues to stress levels in relation to strength levels).

## Characterizing surface exposures with examples

In Nordic countries in particular, where glaciation has exposed a lot of rock, it is possible to gain a good assessment of the higher end of the rock quality scale and likely best tunneling conditions, by observing and mapping surface exposures. When road cuttings are also available, the rock conditions in these better rock-quality terrains can also be readily mapped. However, seismic refraction measurements (next section) and dedicated deviated drilling of low velocity weakness zones will be needed where exposures are absent in flatter and lower areas. These low-relief areas may nevertheless be tunneled under, such as in the case of future high speed railway tunnels. One of these projects is about to start near Oslo.

More than 300 rock cuttings were Q-logged to obtain rock mass quality input for $Q_{TBM}$ prognoses for these up-coming rail tunnels near Oslo. However this exposure logging gave data of relevance only to the top five rock classes, and seismic results and core logging of weakness zones was needed to provide approximate information on the lowest rock classes. In Figure 4, some examples of exposure logging using the Q-method are illustrated, using a deliberately wide variation in rock mass quality from the Oslo region.

Arguments are sometimes heard in conferences that Norway only has pre-Cambrian granites and gneisses, and therefore excellent tunneling conditions. In fact Norway has some (lower percentage of) extreme tunneling conditions, with quite frequent swelling clay, occasional sand inrushes, rock bursting where high cover, and some extensively sheared and clay-bearing rock masses, requiring heavy support, and the actual need of local concrete lining. There are at least ten named collapsed caldera in the geologic history of today’s Oslo region.

## Additional advice concerning surface exposure logging

- The near surface rocks will often be more jointed than the unweathered rock masses at a greater depth. This may especially be the case in schistose rocks, which often have a tendency to disintegrate near the surface. Frequently only the better quality rock masses are exposed at the surface.
- Exposures in the terrain are often well rounded by the ice in Nordic countries and weathered in other countries, reducing the possibility to see joints undisturbed, therefore making reliable description of roughness Jr and joint filling Ja, rather difficult. The parameter RQD will usually be underestimated from natural outcrops, due to weathering or frost damage, while Jn will tend to be over-estimated. However in competent hard rock which has been rounded by ice, RQD will be over-estimated and Jn will be under-estimated, due to erosion of the more jointed materials.
- In weathered rock, the joints may be hidden at the surface. Hence the Q-values relevant to tunnel depth could in some cases be over-estimated. However, depending on rock type, the quality at depth may often be seriously underestimated using surface exposures, and experience is needed to make relevant adjustments for this.

| | |
|---|---|
|  |  |
| The massive nature of this motorway rock cutting can be judged by the 2m high 'elg fence'. Class 1 granites.$Q_{range} \approx$ (90-100)/(6-9)x(1.5-2)/(1-2)x(0.66-1)/1$\approx$ 5 - 66. Massive, abrasive, hard to bore with TBM. | Drammen granite near Lier Tunnels. Classic three joint-set rock mass. Joints in full sun-light have least favourable Jr/Ja combination.<br>$Q_{range} \approx$ 100/9 x 1.5/(1-2) x 0.66/1 = 6-11. |
|  |  |
| Well-jointed shale close to Oslo tunnel portals. Note closely-spaced half-barrels. The shale was interbedded with nodular limestones of higher quality. $Q_{range} \approx$ (10-20)/9 x 1/(1-2) x 0.66/1 $\approx$ 0.4 – 1.5. | Sheared and clay-bearing hornfels next to granite batholith near Asker along E18 motorway. Examples of three Jr/Ja 'contact' categories.$Q_{range} \approx$(10-30)/(9-12)x(1-1.5)/(4-6)x(0.33-0.66)/5 $\approx$ 0.01-0.2. |

*Figure 4 Rock exposures selected from the Oslo area, mostly connected to tunnels built or planned. Note that in the case of clay-bearing rock, permeability (and water pressure) may be partitioned. High pressures can occur on just one side of a fault zone, until penetrated.*

- In high road cuttings or other excavated slopes, the joint surfaces are normally well exposed after blasting, giving a more reliable basis for estimating RQD, $J_n$, $J_r$ and $J_a$.
- Rock cuttings excavated in different directions, if sufficiently high, give approximately the same Q-values as in a tunnel, but small cuttings in partly weathered rock should be ignored.
- The water leakage in a tunnel, $J_w$, will obviously be difficult to predict from field mapping alone. Water loss tests in boreholes and/or empirical data from projects in similar rock masses are necessary to obtain good predictions of the likely water conditions.
- A prediction of the SRF-value may be made based on the topographic features and knowledge of the stress situation in nearby underground openings in the region. High and steep mountain sides often give an anisotropic stress field.
- Geological structures, such as fractures parallel to the mountain side, and sickle shaped exfoliation, are indications of high, anisotropic stresses. The limit for exfoliation in high mountain sides or spalling in a tunnel is dependent on the relation between induced stress and the compressive strength of the rock. In hard rock this limit normally occurs between 400 and 1100 m rock cover above the tunnel. This depends on the compressive strength of the intact rock and the gradient of the mountain side.

- Stress measurement within drill holes may be carried out before tunnel excavation in some of the larger tunnelling or hydropower projects, and this makes SRF estimation more reliable. Note that stress-induced fracturing referred to above starts when the ratio of the maximum estimated tangential stress compared to uniaxial strength ($\sigma_\theta/\sigma_c$) exceeds about 0.4. This signifies the starting point for considerably increased SRF values. This experience is confirmed in mining and in deep road tunnels.
- Mapping for subsea tunnels is limited to the outcrops which are visible on both sides of the strait or fjord under which the tunnel is planned. For subsea tunnels use of seismic techniques is therefore even more important. Core drilling from the shoreline or islands are carried out. Deviated and steered drill holes up to 1000m long may be used for seabed to borehole seismic tomography. More seldom, because of the expense, core drilling from a ship may be carried out. This will be done for the 27km long planned Rogfast subsea (-390 m) road tunnel, which will be the world's longest road tunnel.

## Using seismic velocity and Q to interpolate between boreholes

An empirically-based correlation between the Q-value and the P-wave velocity derived from shallow refraction seismic measurements was developed by Barton, 1995 from trial-and-error lasting several years (Figures 5 and 6). The velocities were based on a large body of experimental data from hard rock sites in Norway and Sweden, thanks to extensive documentation by Sjøgren et al. (1979), using seismic profiles (totaling 113 km) and local profile-oriented core logging results (totaling 2.85 km of core). The initial $V_P$-Q correlation had the following simple form, and was relevant for *hard rocks with low porosity*, and specifically applied to shallow refraction seismic, i.e. 20 to 30m depth, as suggested by Sjøgren.

$V_P \approx 3.5 + \log Q$   (km/s)   (2)

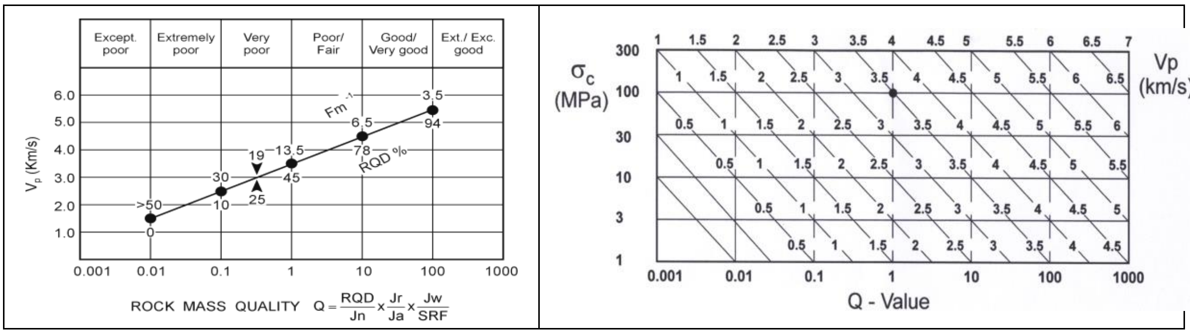


*Figure 5 Left: Hard rock, shallow seismic refraction mean trends from Sjøgren et al. (1979). The Q-scale was added by Barton (1995), using the hard rock correlation $V_p \approx 3.5 + \log Q$. By remembering Q = 1: Vp ≈ 3.5 km/s, the Q-Vp approximation to a wide range of qualities is at one's fingertips (e.g. for hard, massive rock: Q = 100: Vp ≈ 5.5 km/s). Right: Generalization to include rock with different $\sigma_c$ values.The results still apply to shallow seismic.The source of this figure is explained in Barton, 2006.*

A more general form of the relation between the Q-value and P-wave velocity is obtained by normalizing the Q-value with the multiplier UCS/100 or $\sigma_c/100$, where the uniaxial compressive strength is expressed in MPa ($Q_c = Q \times \sigma_c/100$). The $Q_c$ form has more general application, as weaker and weathered rock can be included, with a (-ve) correction for porosity.

$V_P \approx 3.5 + \log Q_c$  (km/s)   (3)

The derivation of the empirical equations for support pressure (originally in Barton et al. (1974) and for the static deformation modulus (in Barton 1995, 2002) suggest an approximately inverse relationship between *support pressure needs* and rock mass *deformation moduli*. This surprising simplicity is not illogical. However it specifically applies with the mid-range Jr = 2 joint roughness.

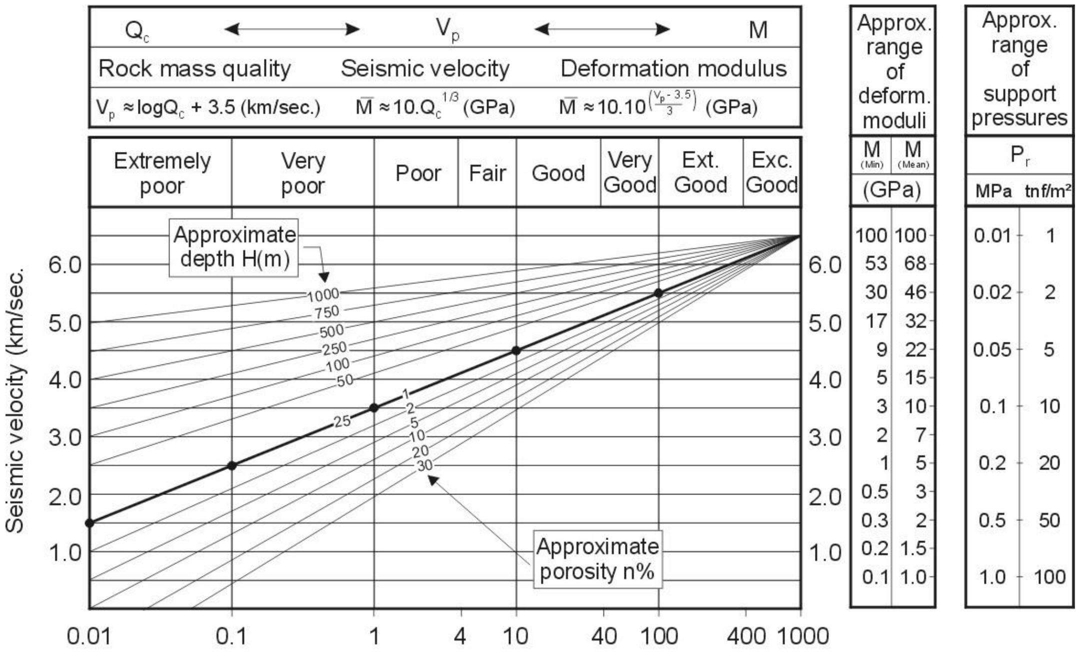


$$Q_c = \left[ \frac{RQD}{J_n} \times \frac{J_r}{J_a} \times \frac{J_w}{SRF} \right] \frac{\sigma_c}{100}$$

*Figure 6 The thick ‘central diagonal’ line is the same as the sloping line given in Figure 5, and this applies to nominal 25-30m depth shallow seismic refraction results. In practice the nominal 1% (typical hard rock) porosity would be replaced by increased porosity if rock was deeply weathered, and the more steeply sloping lines (below the ‘central diagonal’) would then suggest the approximate (-ve) correction to $V_P$. Note that very jointed rock with open joints may have lower velocity than saturated soil. The less inclined lines above the ‘central diagonal’ represent greater depth (50, 100, 250m etc), and these lines correct $V_P$ for documented stress or depth effects (+ve). These depth-lines were derived from several sets of deep cross-hole seismic tomography, with Q-logging of the respective cores (Barton, 2002). Note the inverse nature of (static) deformation moduli and support pressure shown in the right-hand columns. These derivations are described in Barton (1995) and Barton (2002). For a more detailed treatment of seismic, for example the effects of anisotropy which are accentuated when the rock is dry or above the water table, refer to the numerous cases illustrated and summarized in the text book of Barton (2006).*

## Characterizing the rock mass in tunnels by inspecting each tunnel advance

The final role of the Q-system is to document the rock mass quality of each advance of the tunnel, and thereby assist in the selection of the final support (Sfr) and reinforcement (B) class. This cannot be done by infrequent finite element modelling or rejection of the empirical method, as suggested by some recent authors in Germany, Austria, Switzerland and Canada. Steel-fiber (or polypropylene) reinforced shotcrete and systematic, corrosion-protected rock bolts (B + Sfr) form the usual Norwegian single-shell tunnel (or cavern) ‘lining’. There is infrequent use of rib-reinforced shotcrete (RRS), and occasional cast concrete (CCA) in short sections of bad rock. All of these measures are selected with the help of the Q-support chart (see next section). However, special conditions may demand special measures, so general Q-based methods may be modified when necessary. This will be discussed in the next section.

In Norway, following occasional adverse experiences in the past, what has become known as ‘the Owner’s half-hour’ is allotted to thorough rock mass inspection and characterization. The idea is that engineering geologists representing the Owner and Contractor can each log Q.

| | |
|---|---|
|  |  |
| Rock mass classification has to be done close to the crown, using a hydraulically raised cage, mounted on the drill jumbo. It is easy to overlook altered rock and clay when too far below the arch in large tunnels. | Inspection of initial shotcrete (Sfr) support must also be carried out from high in the tunnel arch, using a crowbar to check for 'drumminess'. Poorly bonded areas due to insufficient jet-washing need repair. |
|  |  |
| Three joint sets ($J_n$ = 9), planar and rough-surfaced ($J_r$ = 1,5). Sandstone in the Bremanger tunnel in Western Norway. Note that the location with over-break with three well-developed joint sets attracts Q-loggers attention, but may be more jointed than elsewhere. $Q_{range} \approx (30\text{-}80)/(6\text{-}9) \times 1.5/1 \times 1/1 \approx 5\text{-}20$.. | Shallow cavern, with weathering or clay coatings on several of the joint sets. The granite has high RQD (90-100%) and large block sizes. This emphasizes need for additional Q-parameters to reflect the lower quality. Serious over-break due to critical ratio of $J_n/J_r \geq 6$. $Q_{range} \approx (90\text{-}100)/9 \times 1.5/(2\text{-}4) \times 0.66/2.5 \approx 1\text{-}2$. |
|  |  |
| Stress-induced fracturing in marble in the walls of the Jinping I headrace tunnels, where two large-diameter TBM were eventually removed, due to > 2 km cover. Completion by drill-and-blast: total of four // tunnels. $Q_{range} \approx (90\text{-}100)/(2\text{-}3) \times (2\text{-}4)/1 \times (0.5\text{-}1)/(50\text{-}200) \approx 1$. | Tunnel face in (pre-injected) shales. Note first layer of S(fr) and permanent (CT) bolts close to previous face. A conservative 3m advance. In fact the prior quality of the shales has been improved by 10 MPa pre-injection. $Q_{effective}$ has improved from ≈ 1 to 30. |

*Figure 7 Some figures to illustrate tunnel inspection needs following blasting and prior to final support and reinforcement decisions. Some diverse tunnel Q-value estimates are also given.*

If conditions permit, this is done before temporary or permanent support and reinforcement operations are commenced, following the last advance of e.g. 2 to 5m. This ‘half hour’ is reserved (and fully costed) so that the engineering geologist representing the contractor, and the engineering geologist representing the owner, can jointly try to come to agreement about the quality (or lack of quality) of the newly exposed rock mass. Having a standard method like the Q-system, and time for discussion, adds to the reliability, and both engineering geologists learn from each other. Shift work for the project engineering geologists is obviously needed when tunneling is progressing during two or more shifts each 24 hours.

The structural-geological (rock-type and joint-set recordings) and Q-logging is of course done following blast-gas displacement, and following scaling (‘barring-down’) by the contractor. The fact that wet-process shotcreting is used, as opposed to dry-process methods, plus the relatively small number of operatives and vehicles in Norwegian tunnels, means that air quality is generally superior to what is experienced in many other countries. This makes rock mass inspection easier and it is therefore more likely to be correct. Single-shell tunneling demands this reliability. Some examples of Q-logging in tunnels were illustrated in Figure 7.

Because tunnel cross-sections can be quite large, and because full-face blasting is common (and sounder practice) where rock quality allows this, the height of the tunnel arch usually means that rock mass inspection from a hydraulically-lifted and well-lighted cage is imperative. The rock mass quality (especially the lack of quality) is much more likely to be seen when close to the rock surface. Features such as clay-filled discontinuities are less likely to be missed. Geological hammers and a readily available scaling-bar to extend reach and avoid too-frequent moving of the cage, are obvious features of this inspection and decision-making. While some consulting companies may have performed numerical modelling of representative rock mass and tunnel support classes, now is the time to decide which support class and not wait for external decisions. This is important when 40 to 80m per week per face is the typical range of advance rates of single-shell NMT excavations.

There have been two deservedly much-publicised road tunnel rock-falls in the last 20 years in Norway, fortunately with no injuries or fatalities involved. Both have involved incorrect application of the Q-system, with an error in one case of assuming Q =70, while independent engineering geologists recorded Q=0.07 after the event, obviously with the benefit of hind-sight, including post-failure observation. In other words there was a 1000:1 error in the Q-estimate, due to failure to recognise a clay-infested section of a sub-sea tunnel, due to inadequate arch inspection and Q-logging routines.

## Effect of orientation of geological structures on Q-value

Over the years many have commented on the *apparent* lack of discontinuity orientation in the derivation and application of the Q-value. Unlike the case in RMR, there is no specific term for an ‘orientation rating’. Nevertheless there is the instruction to try to consider the least favourable joint set or discontinuity from the point of view of over-break potential or instability, when selecting the appropriate Jr/Ja ratio. This aspect of Q-logging sometimes requires significantly more experience than required when using RMR, because one needs to vizualise the consequences of continuing tunnel advance in case of not providing specific ‘feature’ support. Prior 3D (e.g. 3DEC) modelling of such cases might have been performed.

Figure 8a shows two cases which can be used for illustration. On the left is a small detail from one of Norway’s numerous headrace tunnels. A graphite-coated minor fault strikes sub-parallel to the tunnel axis, while perpendicular to the axis is a set of chlorite coated joints. If considered individually the respective Jr/Ja ratios would be 1.5/3 and 2/4 respectively. The graphite-coated feature follows the tunnel axis for many meters, and is the chief cause of over-break and significant potential instability. Even if the Jr/Ja ratios had not been equal, the Jr/Ja = 1.5/3 combination applies in this case, while the more stable perpendicularly oriented feature with Jr/Ja = 2/4, merely contributes to a lower RQD.

In the case of the unsupported portal of the old coastal road tunnel shown in Figure 8b, the smooth sub-vertical joint set with strike sub-parallel to the tunnel axis should have supplied the appropriate Jr/Ja ratio of 1/2. With a local portal rock mass quality of 100/(9x2) x 1/2 x 1/2.5 ≈ 1 (note: 2 x Jn and SRF = 2.5 for portals) one would expect B of 1.7 m c/c and 7 cm of S(fr) (see next section), if the tunnel had come under today's Q-support decision-making. However, the tunnel has existed for a long time without support, so the Q-system is seen to be conservative, if correctly applied. Some numerical modellers do not seem to agree here. Of course there are good reason for this when modellers make all joint sets continuous.

*Figure 8 a and b  Some specifically oriented details in a headrace tunnel in granite and in an old road tunnel along the west coast of Norway in massive schist. The discontinuity or joint set most adverse-for-stability gives the appropriate Jr/Ja ratio, and extra support may be longitudinally extensive.*

## Tunnel support recommendations based on Q – some history

The Q-system was originally developed from more than 200 case records, which were mostly Scandinavian or of international origin. The single-shell support methods in the early seventies were B + S(mr), i.e. systematic bolting and mesh reinforced shotcrete. The table of support recommendations was based on the location of the case record in 'span-versus-Q' space, as illustrated in Figure 9a, from Barton et al. (1974). With the gradual addition of 1050 more case records by Grimstad, the support and reinforcement recommendations were simplified to the graphic method shown in Figure 9b, from Grimstad and Barton (1993).

In the original Barton et al. (1974) version of Q, rock support and rock reinforcement recommendations were 'separated' by the conditional factors RQD/Jn (i.e. relative block size) and Jr/Ja (i.e. inter-block shear strength). In other words, smaller block sizes (and lower cohesive strength) apparently (and logically) required more S(mr), while lower internal friction apparently (and logically) required closer rock bolt spacing. Later it was discovered (Barton 2002) that Q, or more specifically $Q_c$ closely resembled the multiplication of 'c' and 'tan φ'. This 'semi-empirical' (*a posteriori*) derivation of the two strength components of a rock mass differs greatly from the *a priori* complex algebra of the Hoek-Brown GSI-based rock mass 'strength criterion' (Barton 2014), which so many young people use with continuum finite element modelling, obtaining apparent tunnel 'behaviour' which they believe to be true.

As discussed later, it is wise to combine empirical methods with numerical methods if one wishes to 'design' tunnel support based on numerical modelling. The often exaggerated 'plastic' zones seen in numerical models, and the numerically modelled deformation need to be viewed with suspicion, and sometimes corrected, by empirical Q-deformation data. A very simple method will be illustrated later. Empirical near-reality is closer than *a priori* modelling.

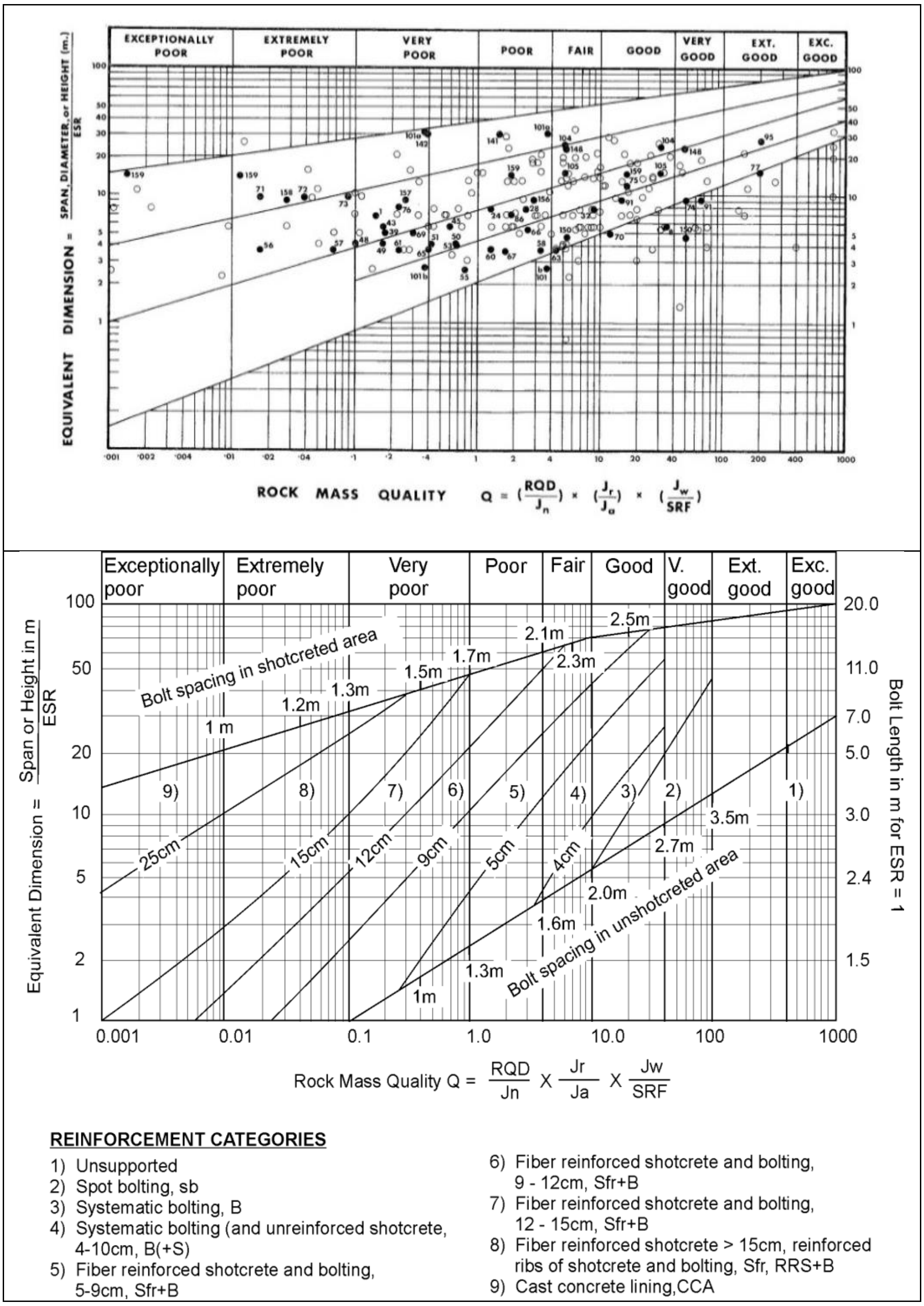


*Figure 9 Top: The Barton et al. (1974) Q-based support chart, with each of the (38) boxes having a separate support and reinforcement recommendation. There were 212 case records, and at this time the standard single-shell method was B+S(mr) – i.e. bolting and steel mesh reinforced shotcrete. By about 1983 S(mr) had gone out of use as a tunnel support measure in Norway, after the development of robotically-applied wet process S(fr) in 1978/1979. Note that the SPAN (the width of the tunnel or cavern) is divided by a 'tunnel-use' safety requirement number ESR, shown later. Bottom: the Grimstad and Barton (1993) tunnel support and reinforcement chart, which was based on some 1,050 new case records. This chart gave permanent single-shell support and reinforcement, also for large caverns. As will be noted later in Figure 13, some small adjustments to minimum shotcrete thickness were made in 2006, described in Grimstad (2007), based on experiences from 800 new cases assembled in 2002/2003. In addition in Figure 13, the RRS (rib reinforced shotcrete) listed under category #8, is given specific dimensions for a wide range of tunnel sizes and Q-values.*

## The components of Q-system based support : S(fr), CT bolts, and RRS

This section consists of illustrations of some key items of the Q-support recommendations shown in Figure 9: including yesterday's S(mr) and the last thirty years S(fr). Photographs and figures are used for reasons of brevity and stand-alone completeness.

Because the Q-system was developed in 1973, the single-shell case records had permanent shotcrete support and bolting reinforcement of lower quality than that available in the decades that followed. This is an example of poor-practice S(mr), with all the disadvantages well illustrated.

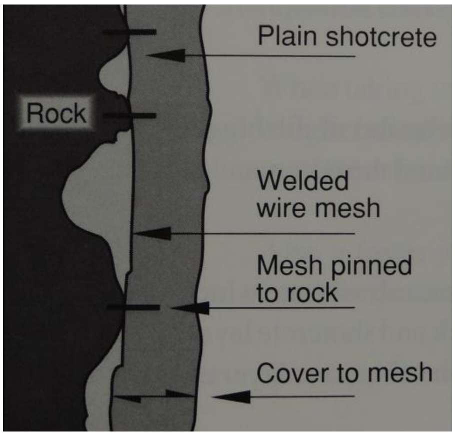


Vandevall (1991) illustration of the pitfalls with mesh reinforced shotcrete: three processes, risk of 'shadow' and /or some rebound, corrosion of the mesh due to electrolytic currents, delayed installation.

Wet process steel-fiber reinforced shotcrete, applied after thorough washing, and use of corrosion-protected rock bolts (e.g. CT-type) are the most important components of the updated Q-system support/reinforcement recommendations. The photograph shows NMT in progress. A final layer of S(fr) completes the support of this pre-injected rail tunnel.

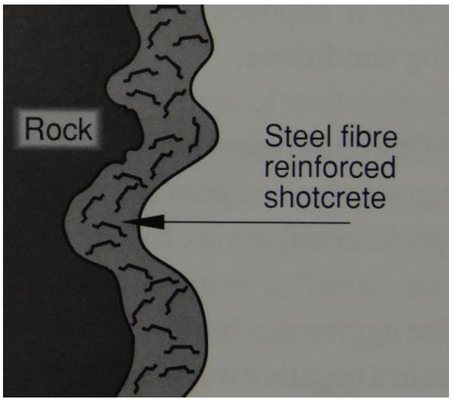


Vandevall, 1991 illustration of the obvious advantages of S(fr): better bonding, no shadow, less corrosion, much lower permeability, faster, cheaper per meter. It is remarkable that some Austrian consultants still recommend S(mr).

*Figure 10 The advantages of S(fr) compared to S(mr) are easily appreciated in these contrasting examples. The sketches from Vandevall (1991) 'Tunnelling the World' are not-exaggerated.*

The reality of single-shell NMT-style tunneling, in comparison to double-shell NATM-style tunneling is that each component of support has to be *permanently relied upon*. There is nothing like the *neglect* of the contribution of temporary shotcrete, temporary rock bolts, and temporary steel sets, and reliance on a final concrete lining, as in NATM. Thus more care is taken in the choice and quality of the support and reinforcement components B+S(fr) + (eventual) RRS. Figure 10 (bottom) illustrates application of S(fr). Figure 11 illustrates (in the form of a shortened demo) the workings of the CT bolt. And finally Figure 12 illustrates some of the internal reinforcement details and final appearance of RRS (rib reinforced shotcrete).

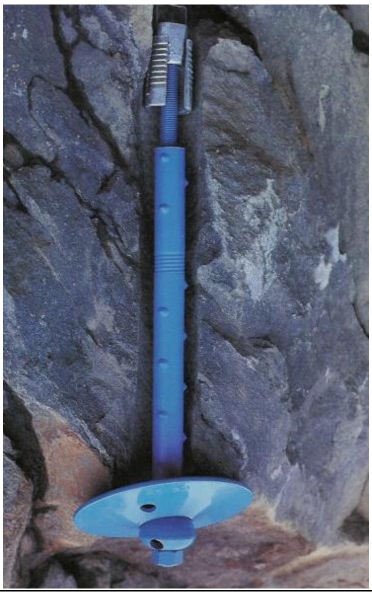

Over-cored CT bolt: Joint/crack deformation next to the bolt (an expected mechanism when installing close to the tunnel face) does not initiate a potential process of corrosion which it might in the case of a conventional bolt without the PVC sleeve.

*Figure 11  Because single-shell (NMT) relies on high quality S(fr) and long-life rock bolts, the multi-layer corrosion protection methods developed by Ørsta Stål in the mid-nineties, became an important part of NMT. The left photo shows a blue-coloured PVC sleeve: the PVC can be black or white.*

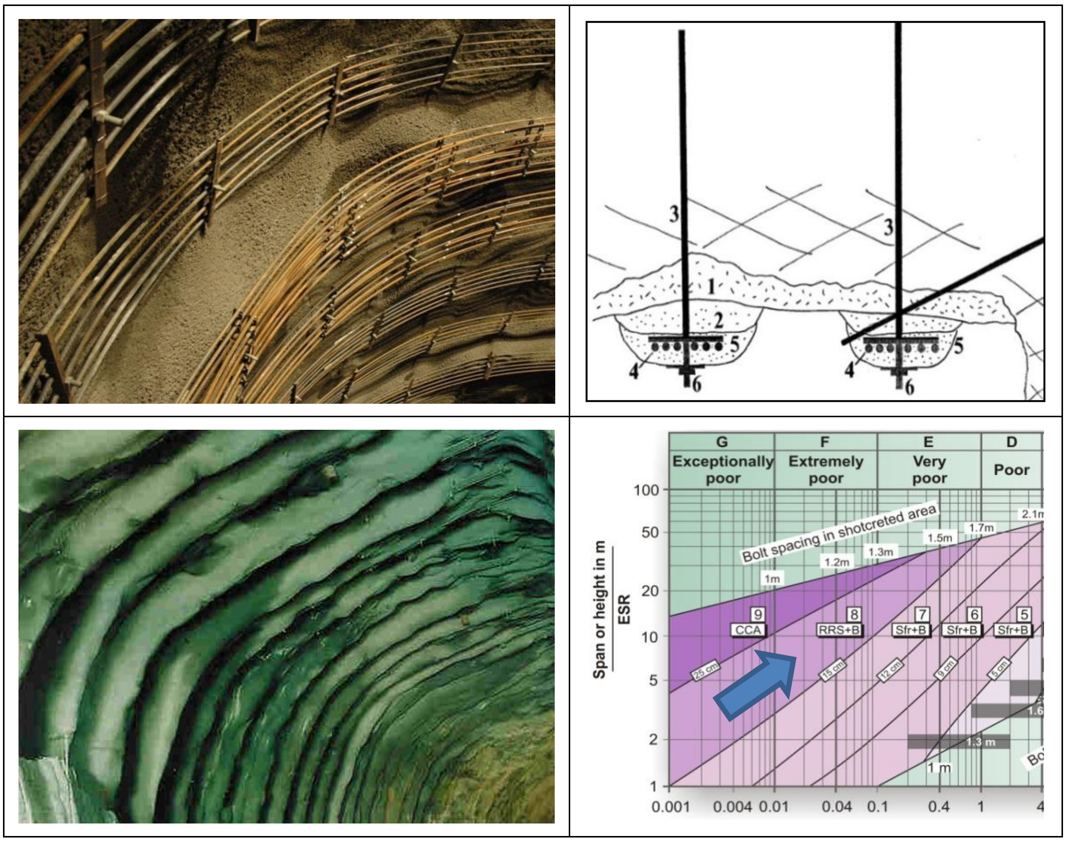


*Figure 12 Some details which illustrate the principle of RRS, which is an important component of the Q-system recommendations for stabilizing very poor rock mass conditions. The top left photograph is from an LNS lecture published by NFF, the design sketch is from Barton (1996), the blue arrow shows in which part of the Q-chart the RRS special support-and-reinforcement measure is 'located' (see greater detail in Figure 13). The photograph of completed RRS is from one side of the National Theater station in downtown Oslo, prior to pillar removal beneath only 5m of rock cover and 15m of sand and clay. Final concrete lining followed the RRS for obvious architectural reasons.*

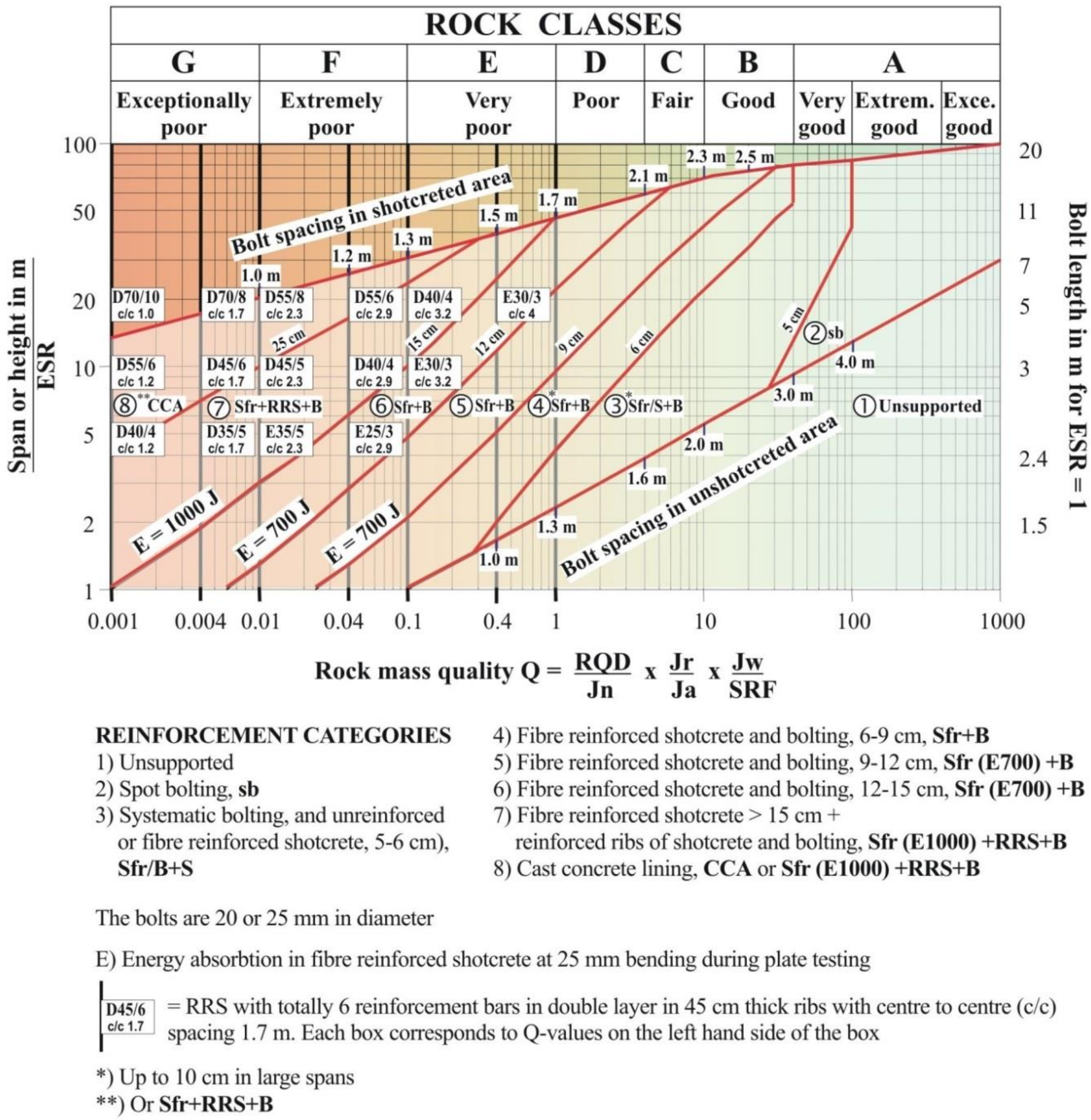


*Figure 13 The updated Q-support chart first published by Grimstad, 2007.The details of RRS dimensioning given in the 'boxes' in the left-hand-side of the Q-support diagram were derived by a combination of empiricism and some specific numerical modelling by a small team of former NGI colleagues. Details of this modelling are given by Grimstad et al. (2002, 2003). Note that each 'box' contains a letter 'D' (double) or a letter 'E' (single) concerning the number of layers of reinforcing bars.(Figure 12a shows both varieties). Following the 'D' or 'E' the 'boxes' show maximum (ridge) thickness in cm (range 30 to 70 cm), and the number of bars in each layer (3 up to 10). The second line in each 'box' shows the c/c spacing of each S(fr) rib (range 4m down to 1m). The 'boxes' are positioned in the Q-support diagram such that the left side corresponds to the relevant Q-value (range 0.4 down to 0.001). Note energy absorption classes E=1000 Joules (for highest tolerance of deformation),700 Joules, and 500 Joules in remainder (for when there is lower expected deformation). Note: use S(fr) to form the arch below the steel bars. Note (from Barton et al. 1974) that bolt length (right-side of Figure 13) is estimated from: L = 2 + 0.15 SPAN/ESR (m). For walls L = 2 + 0.15 HEIGHT/ESR (m). For large caverns with eventual cable anchors, the factor 0.15 is replaced by 0.4 in each case. Note that HEIGHT refers to the full excavation height. See updated ESR values (Table 3).*

It should be noted that the 1993 Q-support chart (shown earlier in Figure 9) suggested the use (at that time) of only 4-5 cm of *unreinforced* sprayed concrete in category 4. The application of *unreinforced* sprayed concrete came to an end during the 1990's, at least in Norway.

Furthermore, thickness down to 4 cm is not used any longer in Norway, due to the already appreciated risk of drying out too fast when it is curing. The Q-chart from 1993 (Figure 9) and also an updated 2002/2003 version, indicated a very narrow category 3 consisting of only bolts in a 10m wide tunnel when Q was as high as 10-20. This 'bolt-only' practice is not accepted any longer in Norway for the case of transport tunnels. The category 3 in 1993 and 2002/2003 has been taken away in this newest 2007 chart (Figure 13) which was fine-tuned by Grimstad when still at NGI in 2006. However for less important tunnels with ESR =1.6 and higher, only spot bolts are still valid. Hence we may distinguish between transport tunnels (road and rail) and head race tunnels, water supply etc. (See later ESR table).

## NMT single-shell tunneling concept summarized in 1992

Shortly before the publication of the updated Q-system tunnel support recommendations by Grimstad and Barton (1993), a multi-company, multi-author group from Norway (Barton, Grimstad, Aas, Opsahl, Bakken, Pedersen and Johansen) from the companies NGI (2), Selmer, Veidekke, Entreprenørservice, NoTeBy and Statkraft, described the main elements of the Norwegian method of tunnelling, calling it NMT. This was in deliberate competition to the much more expensive double-shell NATM. This two-part article in World Tunnelling (Barton et al. 1992) described Q-logging, numerical modelling, tunnel support selection, robotic application of wet process S(fr), support element properties, and the Norwegian tunnel contract system. The initials NMT are now well known after 20 years referencing and inclusion in university courses outside Norway. This is helpful for distinguishing it from the very different NATM.

*Table 2 An expanded text to explain the NMT abbreviations in the 'drawers' in Figure 14.*

| | |
|---|---|
| ***Rock mass characterization*** *using the six Q-parameters. A relationship between Q and $V_P$ and deformation modulus M is indicated, using $Q_c$, $\sigma_c$, matrix porosity n% and depth H (m) or stress level.* | ***Site investigation*** *using seismic refraction, radar, cross-hole $V_P$ or $E_{dyn}$ tomogram, or attenuation tomogram. (Note $Q_{seismic}$ =1/attenuation is numerically close to M GPa).* |
| ***Support design measures*** *consist of none, sb, B, B+S, B+S(fr), RRS, CCA. (Untensioned grouted $B_{utg}$ bolts, tensioned resin end-anchored bolts, and CT bolts). Also may use spiling, drainage, pre-injection, and freezing.* | ***Numerical verification of support designs*** *using codes like UDEC, UDEC-BB, UDEC-Sfr, FLAC, FLAC-3D and 3DEC. Relevant parameters JRC, JCS, $\varphi_r$, M, Kn and Ks, c + $\varphi$.* |
| ***S(fr) robot technology*** *using Portland cement, silica fume, plasticizer, super-plasticiser, aggregate and non-alkali (low) accelerator. Steel fiber: EE 20-25 mm (previously), Bekaert 30-35mm / 0.5mm. (Today: also PP fiber Barchip 48mm, 0.4 /1.4mm).* | ***Norwegian tunnel contract system*** *uses a flexible contract, with unit prices for all possible measures in tender documents: use the motto 'expect the unexpected'.* |
| ***Rapid advance*** *due to wet process S(fr) shotcrete, gives low rebound and improved environment.* | ***Low cost and*** *less conflicts, permanent single-shell support compared to double-shell NATM.* |

## Concerning bolting and fibre types in the Q-recommendations

- The early Q-system nomenclature $B_{utg}$ shown above refers to *untensioned grouted bolts*, which are very stiff. Their use has to be carefully considered when there is early large deformation, spalling or rock burst. Grouting of end-anchored rock bolts too early may increase the adverse effects of spalling, and bolts may also fail in tension in large numbers. It is better to grout the bolts when deformation has slowed down. A highly recommendable alternative is the use of energy/deformation absorbing D-bolts.
- EE-fibers went out of use in Norway in the mid 1990's. Bekaert steel fibers 30-35mm long, among others, are partially being substituted by polypropylene fibers, such as Barchip Kyodo 48mm long, in some sections of the tunneling industry. However it is rather important that these fibres are rough-surfaced to ensure their anchorage and

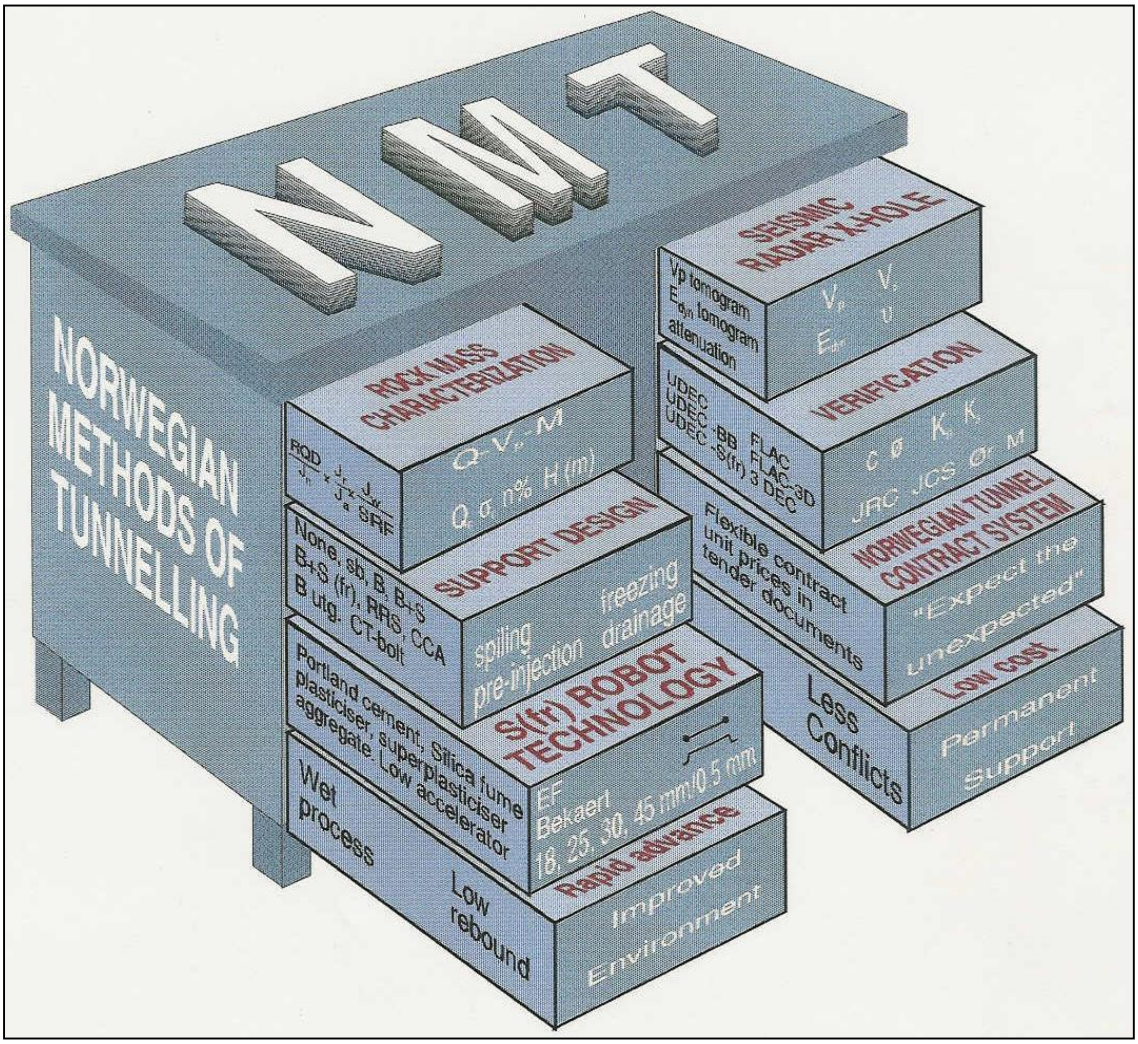


*Figure 14 The 'design-and-execute' tunneller's desk-of-drawers, used by Barton (1996) to summarize key elements of NMT for an international readership. Table 2 gives a summary of the 'content' of each drawer, using added connecting text.*

deformation resistance. The desirable decades-long behaviour of polypropylene fibres is not yet possible to document, but extensive use in parts of the tunneling industry, such as in subsea road and rail tunnels and when large deformation is expected, is a positive signal.

## Contrasting single-shell NMT and double-shell NATM

The use of steel sets is avoided in the practice of single-shell NMT, due to the potential loosening of insufficiently supported rock in the periphery of the excavation. It is difficult to make sufficiently stiff contact between the steel sets and the rock, especially when there is over-break. The results of experiments using different support methods are illustrated in Figure 15. The left-hand diagram shows the results of trial tunnel sections in mudstone (Ward et al.1983). The five years of monitoring clearly demonstrate the widely different performance of the four different support and reinforcement measures.

In the right-hand diagram, from Barton and Grimstad (1994), the contrasting stiffness of B+S(fr) and steel sets is illustrated in a 'confinement-convergence' diagram, with the implication (and reality) that SRF (loosening variety: see APPENDIX A1) may occur when using steel sets. It should be clear that the early application of S(fr) by shotcrete robot, and the installation of permanent corrosion protected rock bolts from the start, as in single-shell NMT, is likely to give a quite different result from that achieved when using NATM.

In the latter, the commonly used steel sets and mesh-reinforced shotcrete and rock bolts are all considered just as temporary support, and are not 'taken credit for' in the design of the final concrete lining. These temporary support measures are assumed to eventually corrode. It is then perhaps not surprising that convergence monitoring is such an important part of NATM, as a degree of loosening seems to be likely when so often using steel sets. The standard procedures involved in NATM are illustrated in Austrian standards, and are reproduced for reference (Figure 18) since so remarkably different to single-shell NMT.

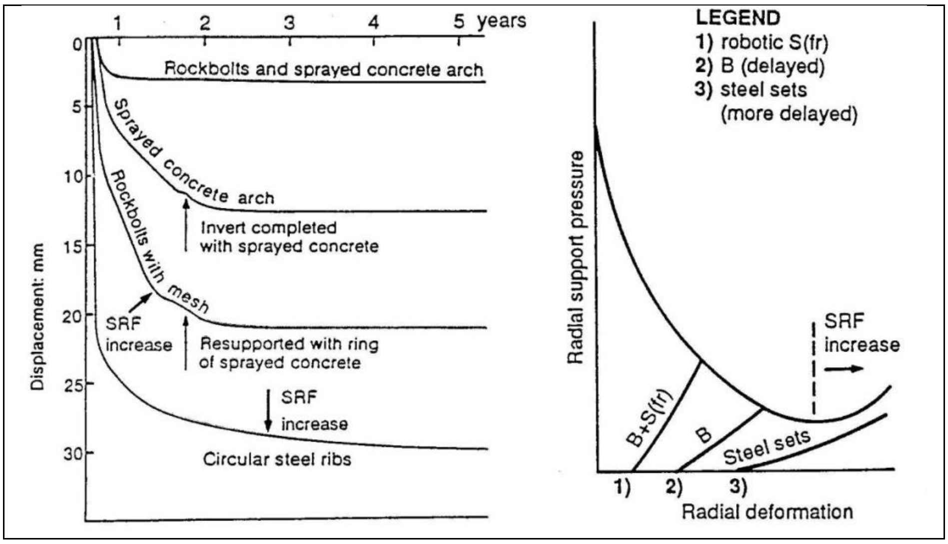


*Figure 15 Left: Results of five years of monitoring test-tunnel sections in mudstone, using four different support and reinforcement measures, from Ward et al. (1983). The obvious superiority of B+S in relation to steel sets is clear. The last 35 years of B+S(fr), as practiced in Norway would presumably give an even better result. Right: Representation of the relative stiffness of different support measures, from Barton and Grimstad (1994). SRF may increase due to loosening in the case of steel sets. See Figure 16, which illustrates the implicit difficulty of controlling deformation with steel sets/lattice girders.*

*Figure 16 Left: An illustration of the challenge of making contact between the excavation periphery and the steel sets, even for the case of limited over-break. In NATM the 'sprayed-in' steel sets, and S(mr) and bolting are considered temporary, and are not included in the design of the final concrete lining. Right: Steel sets are actually a very deformable type of tunnel support. However in squeezing rock as illustrated, the application of RRS might also be a challenge, unless self-boring rock bolts were used to bolt the RRS ribs in the incompetent (over-stressed) rock that is likely to surround the tunnel in such cases.*

*Figure 17 Left: Illustration of a 'missing component' of support. When the rock mass is significantly jointed and with low cohesion, bolting and mesh alone are clearly inadequate. Right: An illustration of the use of temporary steel sets and mesh reinforced shotcrete, both of which potentially invite increased deformation and possible loss of strength. A local collapse and large deformation is shown.*

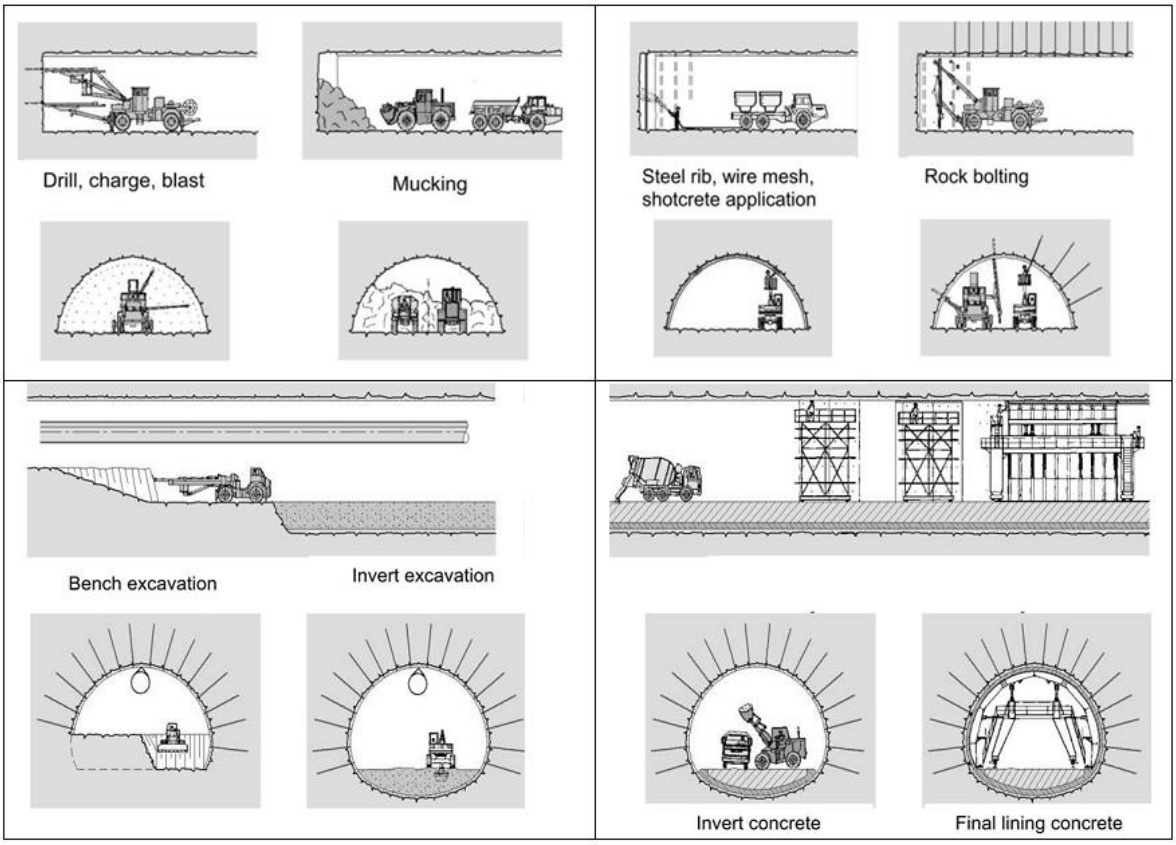


*Figure 18 Schematic construction sequence of a typical NATM tunnel, apparently used in both softer and harder rock, from "Austrian Society for Geomechanics (2010). NATM, 'The Austrian Practice of Conventional Tunnelling'. This method has been observed in many countries when Q is 'poor', 'fair', 'good' i.e. Q = 1 to 40, where NMT would be eminently suitable and much faster and cheaper.*

In contrast to the sequences of NATM shown in Figure 18, in NMT the excavation is usually full-face, both for speed and to avoid a very unfavourable top-heading section (as illustrated in Figure 18). This invites the initiation of invert heave if the tunnel is at significant depth and not in hard rock. Final support in NMT is usually B+S(fr), while in double-shell NATM the final support is only the final concrete lining, which also secures the drainage fleece and membrane. The concrete lining is designed to take all ultimate loads from the rock mass. The temporary steel sets, S(mr), and bolting are assumed in the long-term to have corroded and are not featured in the final concrete load-bearing structure. This design philosophy, which is surprising to many, adds to the time and cost of NATM.

Inevitably the cost difference between NATM and NMT is of the order of 1: 3 to 1: 5, but this depends on rock mass quality, and hence on the type and amount of rock support. The cost difference also depends on differences in labour costs in different countries. There may be a 1:10 difference in the number of tunnel workers involved, and the speed of NATM, including construction of the (3D) membrane and the sometimes locally thick final liner (Barton and Grimstad, 2014) is inevitably much slower than single-shell NMT, due to all the operations, as may be visualized in Figure 18. Those using NATM will often point to poorer rock conditions where NATM tends to be applied. This can be only partly acknowledged, since double-shell NATM procedures are also specified in rock masses of comparable quality to those where NMT would be most applicable. This has been observed in many countries.

Norwegian road and railway tunnels of high standard, with all the technology installed for ventilation, lighting, drainage, safety and communication, cost about 18,000 to 27.000 US $ per meter (road) and about 25,000 to 33,000 US$ per meter (railway), depending on the dimension of the tunnel. International tunneling literature frequently documents 80,000 to 100,000 US per meter for the case of NATM double-shell tunnels.

Concerning tunnelling speed, recent Norwegian world records of 164 m and 173 m in best weeks by two different Norwegian contractors, and a 104 m/week project average for 5.8 km in coal-measure rocks, obviously requiring significant rock support and reinforcement, suggests that NMT is a more efficient process. Figure 19 shows the source of very fast NMT single-shell tunneling; namely the fast cycle time. This is usually below 10 hours for a wide range of Q-values (i.e. 1 to 100), and is as low as 5 to 6 hours at the top end of the rock mass quality scale where support and reinforcement is light or hardly needed.

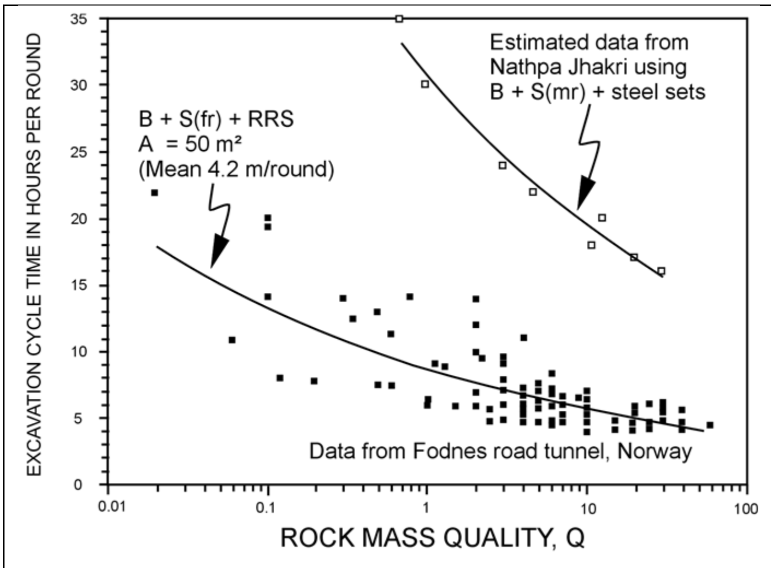


*Figure 19 Cycle-time (drilling blast holes, loading with explosives, blasting, waiting for gasses to clear, scaling, geological inspection, mucking, reinforcement and support) as observed by Grimstad in the Fodnes road tunnel, which has a cross-section of 50-55 $m^2$. For comparison, the cycle-time for labour intensive temporary support methods in a hydroelectric project in India is also shown in relation to the logged Q-values. A final concrete lining will add to the differences in time and cost of NATM compared to NMT.*

### Using the Q-system for temporary support prior to NATM concrete lining

When the Q-system was first published in 1974, it was designed to provide guidance on suitable permanent support for a variety of tunnel and cavern sizes. By way of a footnote, it was suggested that the Q-system could also be used for guiding *temporary support* selection. The suggested rule-of-thumb was '5Q and 1.5 ESR'. This means a diagonal shift, downwards and to the right, on a Q-support chart, as illustrated by the example in Figure 20. This method has been used systematically by Hong Kong road, rail, and metro authorities for at least 25 years, as the preliminary stage of NATM-style tunneling and station cavern development.

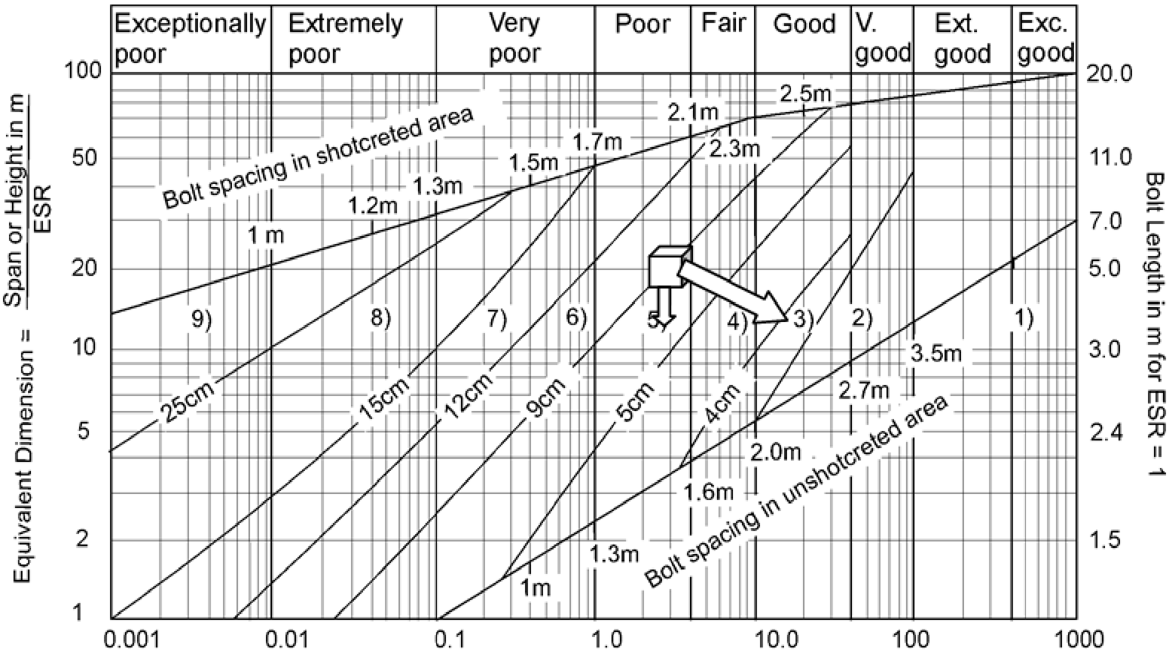


$$\text{Rock Mass Quality } Q = \frac{RQD}{Jn} \times \frac{Jr}{Ja} \times \frac{Jw}{SRF}$$

*Figure 20 Using the 1993 Q-support chart as illustration, the Barton et al. (1974) 'rule-of-thumb' for selecting temporary support is shown for the case of NATM-style tunneling in Hong Kong. Applying 5Q and 1.5 ESR, the span-versus-Q coordinate moves downwards and to the right, ensuring less but sufficient B+S(fr) support while waiting 1 or 2 years for the final concrete lining. The first author has gradually learned to accept this practice when reviewing projects in Hong Kong, but was initially surprised by its widespread use already in the 1990's.*

Table 3 (left-side) shows the ESR values recommended in Barton and Grimstad (1994) for various types of excavation. With the world-wide demand for increased safety in the last two decades, the recommended updated areas of the ESR table are shown on the right. The ESR table published in 1994 was *correct* in the 1970's and in the 1980's. However the demand for safety has increased world-wide and also in Norway, particularly in the case of transport tunnels where small rock falls were accepted in *minor* road tunnels in the 1970's. Now there is no tolerance for any rock falls, even in minor transport tunnels. Minor road and railway tunnels should now have ESR = 1. Water treatment plants with a lot of expensive installations and representing a daily working place should have ESR = 0.9-1.1, and are increasingly more important than storage caverns. Major road and railway tunnels may need ESR= 0.5-0.8. These suggested updates are tabulated on the right-hand side of 1994 values.

*Table 3 On the left the ESR values in use in the nineties (Barton and Grimstad, 1994) are tabulated. Some updates recommended today due to the demand for greater safety are shown on the right (2014). Note the use of italics to emphasise no change from 1994 to 2014.*

| Type of Excavation | | ESR (1994) | ESR (2014) |
|---|---|---|---|
| A | *Temporary mine openings, etc.* | ca. 2-5 | *ca. 2 to 5* |
| B | *Permanent mine openings, water tunnels for hydropower (exclude high pressure penstocks), pilot tunnels, drifts and headings for large openings, surge chambers* | 1.6-2.0 | *1.6 to 2.0* |
| C | *Storage caverns,* water treatment plants, minor road and railway tunnels, *access tunnels* | 1.2-1.3 | 0.9 to 1.1<br>*Storage caverns 1.2-1.3* |
| D | *Power stations,* major road and railway tunnels, *civil defence chambers, portals, intersections* | 0.9-1.1 | Major road and rail tunnels 0.5 to 0.8 |
| E | *Underground nuclear power stations, railway stations, sports and public facilities, factories, major gas pipeline tunnels* | 0.5-0.8 | *0.5 to 0.8* |

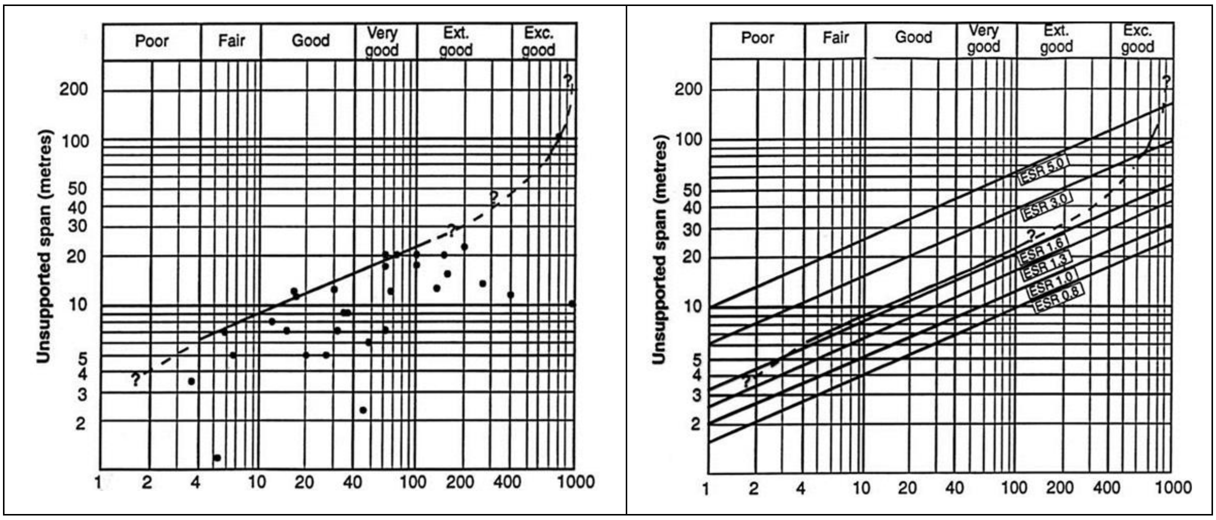


*Figure 21 The workings of ESR, for modifying SPAN to equivalent span The way ESR modifies the equivalent span is shown by the sloping lines, assuming ESR = 1.6 marks the unsupported boundary (for hydropower). (Barton, 1976). Note that 'unsupported span' in the Q-system refers to the width of excavation. In Bieniawski (1989) concerning use of RMR, the 'unsupported span' is the longitudinal distance from the face to the nearest support or reinforcement. These two 'spans' are sometimes confused, due to interest in using the 'stand-up time' chart developed by Bieniawski.*

## RELATIVE TIME AND COST IN RELATION TO THE Q-VALUE

As a result of a survey of some 50 km of tunneling mostly in Norway but also in Sweden, Roald produced the two figures of relative time and cost of tunneling in relation to the Q-value shown in Figure 22. These important trends were subsequently published in Barton, Roald and Buen (2001), in which the main topic was rock mass improvement by pre-injection. In fact this was the first exploration of possible improvements in some of the Q-parameters as a result of high pressure pre-injection. A brief discussion of this topic is given near the end of this illustrated guide on the Q-system.

Figure 22 demonstrates the strong influence of the Q-value on tunneling time and cost. This is independently confirmed using the cycle-time changes with Q, as recorded by Grimstad in a Western Norway road tunnel. This was shown in Figure 19. The general trends shown in Figure 22 concerning relative cost can also be independently derived by a rigid application of the Q-system recommendations for arch and wall support over the whole range of Q-values, and for a wide range of tunnel spans. With knowledge of Q-values, costs can be derived.

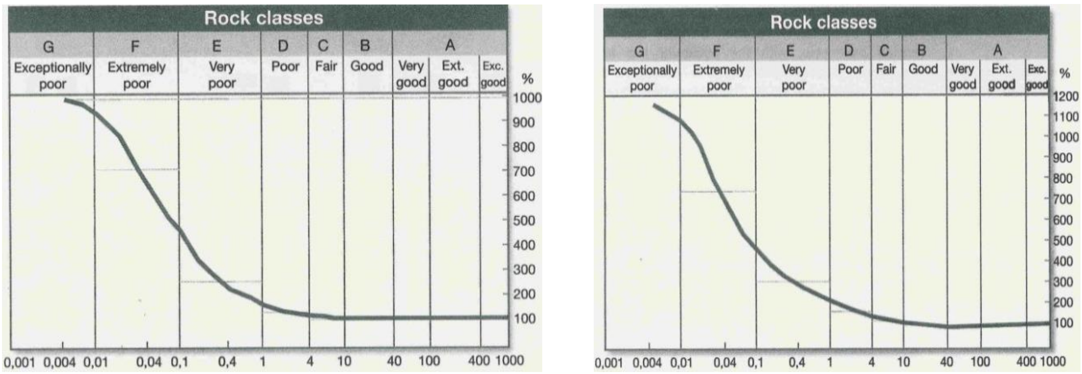


*Figure 22 Relative time (top-left) and cost (top-right) of tunnel construction in relation to Q-value, according to a 50 km survey of tunnels carried out by Roald, and published as Barton et al. (2001).*

## Estimating tunnel or cavern deformation in relation to Q

It appears that the large numerical range of Q (0.001 to 1000 approx.) referred to in the introduction, helps to allow very simple formulæ for relating the Q-value to parameters of interest to rock engineering performance. Figure 23 shows central data trends of $\Delta \approx$ SPAN/Q: a surprisingly simple formulation discovered after receiving the data from Taiwan.

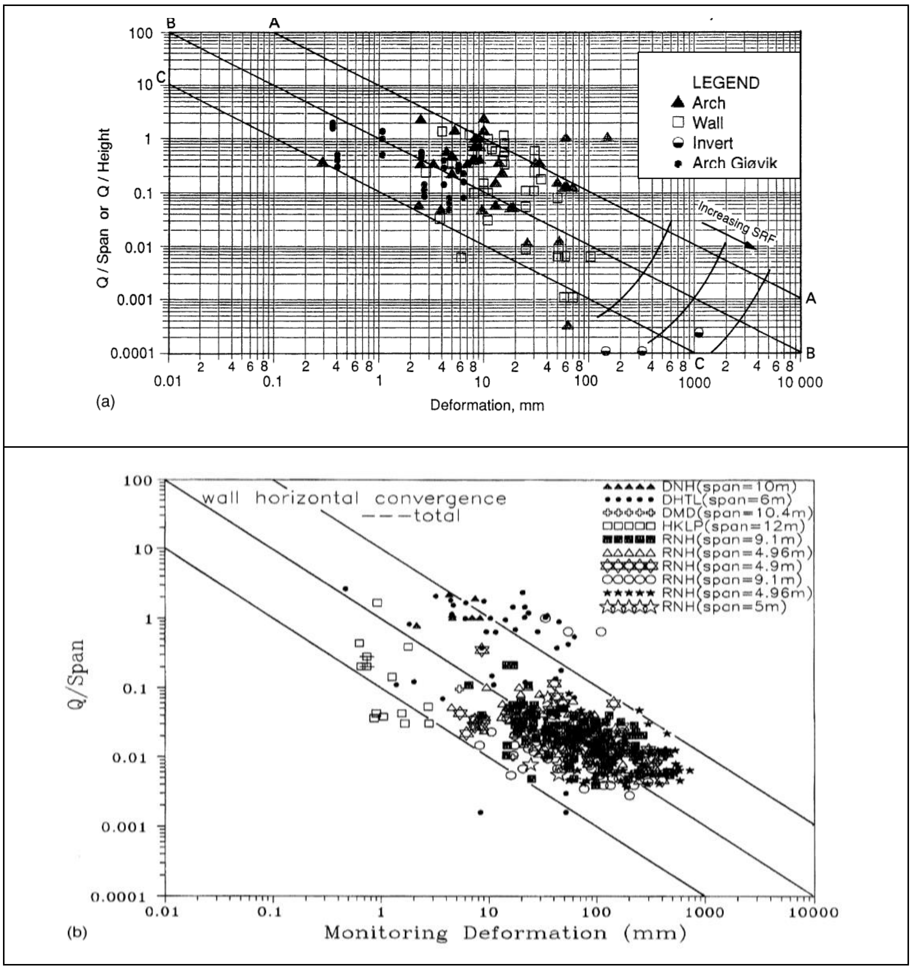


*Figure 23 The log-log plotting of Q/span versus deformation was published in Barton et al., 1994, with fresh data from the MPBX instrumentation of the top-heading and full 60 m span of the Gjøvik Olympic cavern. Shen and Guo (priv. comm.) later provided similar data for numerous tunnels from Taiwan. When investigated, the central trend of hundreds of data was simply Δ (mm) ≈ SPAN (m) /Q.*

*Table 4  Empirical equations 4, 5, 6, and 7 derived from Figure 23, with fine-tuning and reduced scatter using the competence factor stress/strength ratios. Examples of application in Indian and Norwegian caverns. Very close approximation to many cases has been found, including metro station caverns in Hong Kong, where over-continuous jointing in numerical models were showing far too large deformations in relation to the measurements. The empirical equations were again giving good results.*

| | | | |
|---|---|---|---|
| $\Delta = \dfrac{SPAN}{Q}$ | $\Delta_v = \dfrac{SPAN}{100Q}\sqrt{\dfrac{\sigma_v}{\sigma_c}}$ | $\Delta_h = \dfrac{HEIGHT}{100Q}\sqrt{\dfrac{\sigma_h}{\sigma_c}}$ | $k_o = \left(\dfrac{SPAN}{HEIGHT}\right)^2\left(\dfrac{\Delta_h}{\Delta_v}\right)^2$ |

| **Nathpa Jakri power station cavern** | **Gjøvik Olympic cavern** |
|---|---|
| $\Delta_v = \dfrac{20{,}000}{100 \times 3} \times (6/35)^{1/2} = 28$ mm<br>$\Delta_h = \dfrac{50{,}000}{100 \times 3} \times (4/35)^{1/2} = 56$ mm<br>(SPAN = 20m, HEIGHT = 50m, Q = 3, $\sigma_V$=4 MPa, $\sigma_h$ = 6 MPa, $\sigma_C$ = 35 MPa).<br>(In the middle of the range of MPBX measurements for the arch and walls). | $\Delta_v = \dfrac{60{,}000}{100 \times 10} \times (1/75)^{1/2} = 6.9$ mm<br>(SPAN = 60m, $Q_{mean}$ = 10, $\sigma_V$ = 1 MPa at 40 m depth, $\sigma_C$ = 75 MPa)<br>(Almost identical to that measured with nine MPBX, and almost identical to UDEC-BB modelling results). |

## Gjøvik cavern Q-logging, NMT single-shell B+S(fr) support, and deformation

The Gjøvik Olympic cavern was a milestone event in Norwegian rock engineering and rock mechanics practice, combining as it did the experience of several of Norway's leading consulting, research institutes and contracting companies. The Q-system was well utilized, as shown in diagrams c) and d) in Figure 24.

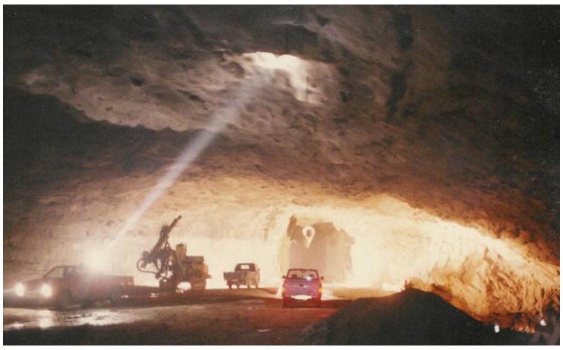

World's largest top-heading waiting for benching-down.

Mean 10 cm of S(fr). Note some  over-break > 1 m.

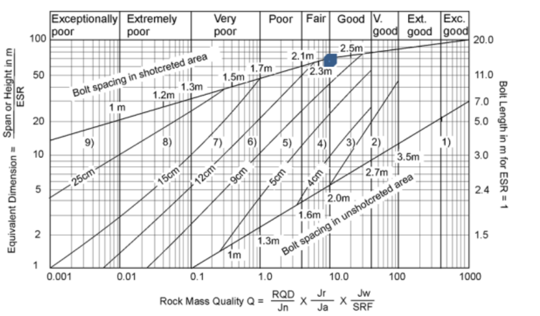


$Q_{mean}$ ≈ 10, span 62m. B 2.5m c/c + S(fr)10cm + cables.

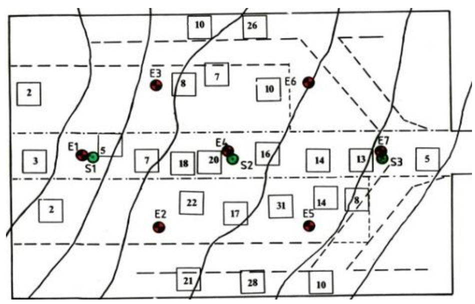

Q-values of arch (boxes): long external MPBX: in red

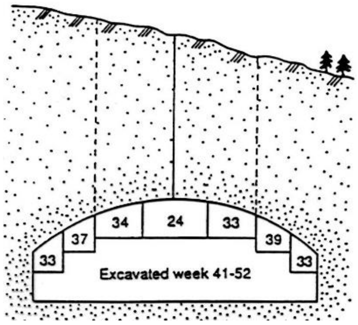


MPBX locations (three rows), excavation week in 1991.

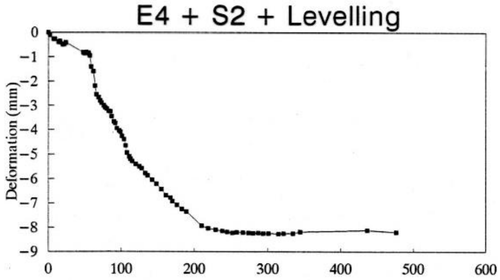


Central deformation 8 mm, ends: 7.0 mm and 7.5 mm

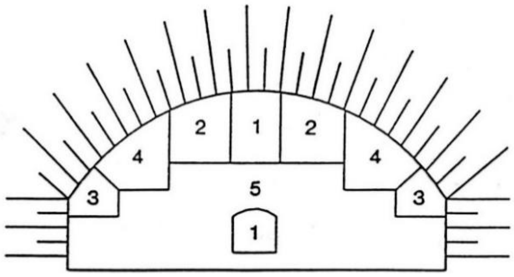


B 2.5m c/c L= 6m, + twin-strand anchors L=12m, c/c 5m

Early games: ice hockey in Winter Olympics of 1994.

*Figure 24 Some details of the Gjøvik Olympic cavern. Concept from Jan Rygh, design studies by Fortifikasjon and NoTeBy, design check modelling with UDEC-BB, external MPBX, seismic tomography, stress measurements and Q-logging by NGI, internal MPBX, bolt and cable loads, modelling, research aspects by SINTEF-NTNU. However, most important of all: efficient construction in 6 months using double-access tunnels, by the Veidekke-Selmer JV. The cavern is an example of a drained NMT excavation. Details of the rock engineering and rock mechanics aspects of the project, including the predictive (Class A) numerical modelling, are given in the multi-author paper of Barton et al. (1994).*

The efficient cavern excavation and execution of single-shell NMT-style permanent support, which took just 6 months in 1991, saw the removal of 140,000 $m^3$ of red and grey gneiss. RQD was mostly 60-90%, and the mean UCS was 90 MPa. The 62 x 24 x 90 m raw-cavern dimensions represented a large (almost 100%) jump in the world's largest-span cavern for public use, with capacity for about 5,400 people for artistic events, concerts etc., which both preceded the winter Olympic ice hockey events of 1994 (i.e. the grand opening ceremony), and have frequently followed in the years since then.

Four boreholes were used for site investigation, two of them inclined. These holes were used for Q-logging (Figure 26a), seismic tomography ($V_P$ range was 3.5 to 5.5 km/s), with the high velocities due to the 30 to 50m deep 3 to 5 MPa horizontal stress.

Representation of the conjugate jointing, the favourably high boundary stresses, the depth-dependent deformation modulus and the eight principal excavation stages used when UDEC-BB modelling the Gjøvik cavern are shown in Figure 25. The modelled vertical deformations above the main arch were approximately 4 and 5 mm depending on the modelled depth of 30 or 50m (relevant to each end of the cavern). The third model shown in Figure 25 had unchanged input data, but included the three Postal Service caverns on the 'right-hand' side (excavation stages # 6, 7 and 8). These caused the central arch vertical deformation to increase to 7 mm. The MPBX-measured results (Figure 24 f) incorporating internal (SINTEF) and external (NGI) extensometers, plus the results of surface levelling (downwards rather than upwards) were 7 to 8 mm.

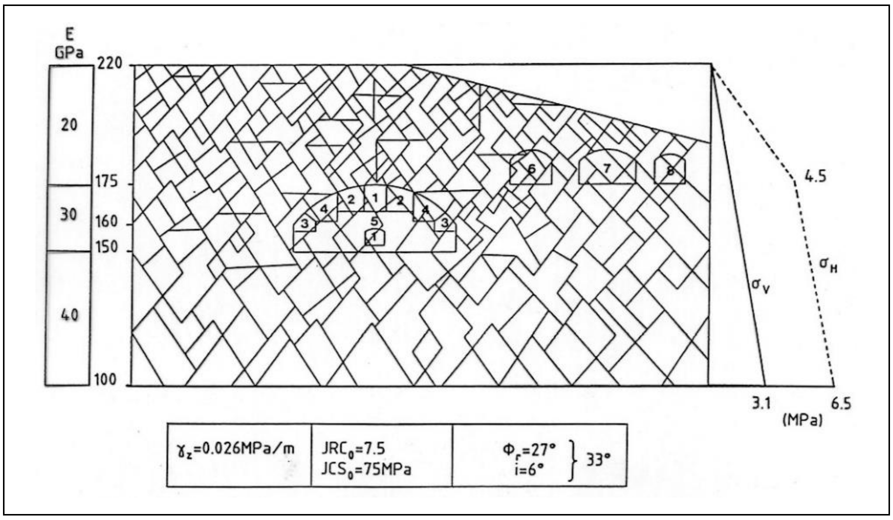


*Figure 25 The geometry of the Gjøvik cavern(s), the excavation stages, the depth-dependent deformation moduli, and the joint properties used in UDEC-BB.* See *Barton et al. (1994) for details.*

Note that the assumptions of joint continuity in this model are far different from the 'lazy modelling' that one sees so often, in which all joint sets are made continuous (for simplicity). Modelled deformations are then much too large, and their authors therefore feel it necessary to criticize empirical methods, when in fact they have grossly over-estimated the deformations and 'plastic zones' due to unrealistic representation of the structural geology.

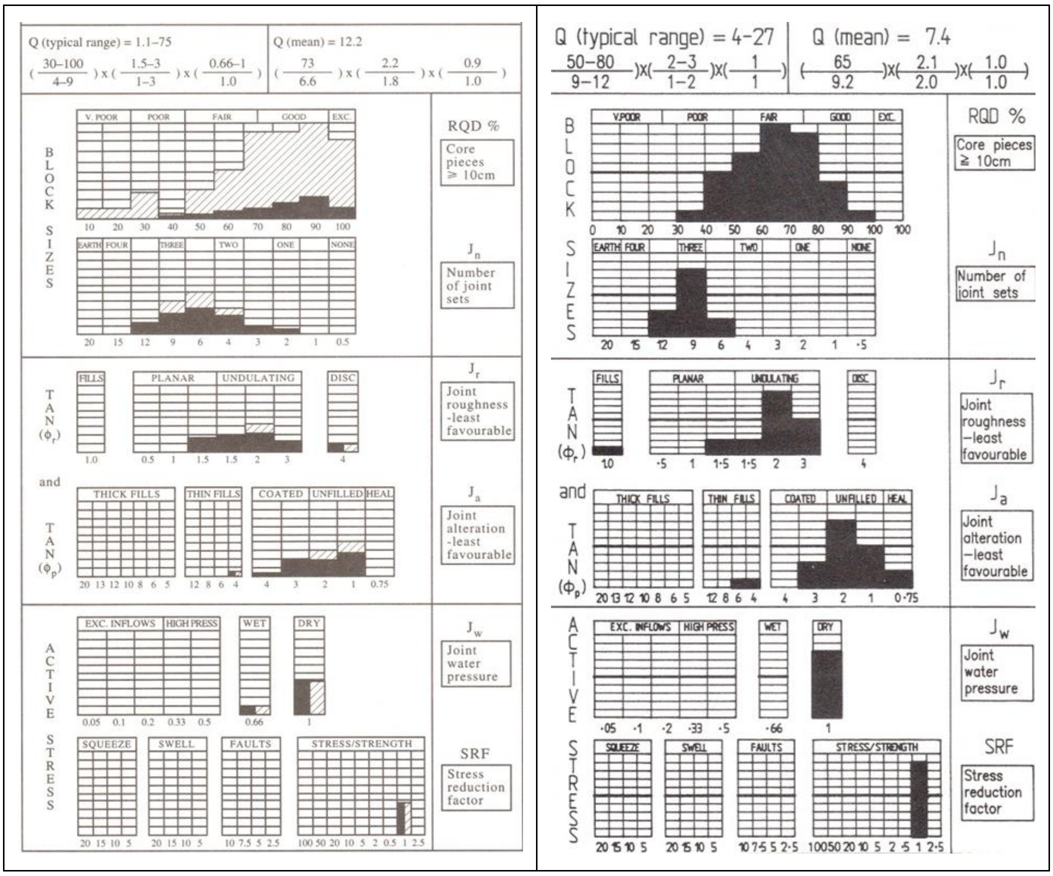


*Figure 26 A comparison of three stages of Q-logging. Left: core-logging (cross-hatched) and local cavern-walls logging (black: where no shotcrete cover). Right: Gjøvik cavern top-heading logging. Three different engineering geologists were responsible for this independent Q-histogram logging.*

## Further Q-system applications – pre-grouting can change effective Q-values

Barton, Roald and Buen (2001) and Barton (2002) suggested, controversially as with most innovations, that several, perhaps most,of the Q-parameters could, *in effect* be improved by the typical high pressure 5 to 10 MPa pre-injection of micro-and ultrafine cements-with-microsilica, as regularly practiced in Norway. This suggestion seems to have been proved correct over time, as some others working in dam foundation engineering and mining are also reporting such finds.

The first author systematically Q-logged all the drill-core and analysed all the permeability measurements for the Jong-Asker and Bærum rail tunnels for JBV (Jernbaneverket). Subsequent experiences suggest that some of the (consultant stipulated) inflow requirements for the first two Jong-Asker tunnels were not stringent enough: due care was taken of the external natural (and built-on) surface environment, but some of the pre-grouting was not sufficiently effective for the inside-the-tunnel environment. Dripping water remained in places, when the least stringent 8 to 16 litres/min/100m inflow criteria were used. However, in the case of the later Bærum rail tunnel of 5 km length, which was systematically injected using more holes and consistently high pressure, a very dry result was obtained. Several inspections of the pre-injected new rounds of tunnel advance suggested that the consultant's single-shell NMT final support, as seen in Figure 27, was now very conservative.

*Figure 27 The pre-injected nodular-limestones and shales of the Bærum Tunnel appeared to have increased in Q-class (by two or three classes) due to the effect of high-pressure pre-injection. Top-left: the first 5 cm layer of S(fr) and the permanent CT bolts-and-washers at approximately 1.5 m c/c. Top-right: bolt heads and washers sprayed in with the final 5 cm layer of S(fr). The tunnel now has its completed single-shell NMT support and reinforcement, which appears to be conservative. The quality of the shale/limestone (and igneous dykes elsewhere), appears to have been improved by the high pressure pre-injection.*

In relation to the extensive (kilometers) of Q-logged core, logged to depths greater than the tunnel depths, there appeared to have been an improvement in the rock mass quality due to the pre-grouting. Not only was the shotcrete 99.999% dry, but the B+S(fr) which was applied, based on prior Q-based designs by other consultants, seemed to be conservative. This can be concluded just by inspecting the photographs in Figure 27 which are typical of many.

Table 5 shows two hypothetical models for 'before-and-after' Q parameter improvements, to illustrate the possibilities. The pre-grouting models have no relation to the two Bærum tunnel photographs, and were presented by Barton (2011/2012). Reduced tunnel support needs, reduced deformation, increased deformation modulus and increased seismic velocity as a result of pre-grouting (the latter documented in Barton, 2006) are each suggested. Naturally one expects as a very minimum that a Jw of 0.5 or 0.66 will become 1.0 ('dry') as a result of successful pre-injection. Other parameters seem also to benefit, including the *effective*

*Table 5 Two hypothetical but not unrealistic 'models' for potential Q-parameter improvement as a result of pre-injection. Barton (2011/2012).*

| | |
|---|---|
| ***CONSERVATIVE* PRE-INJECTION MODEL** | ***MORE REALISTIC* PRE-INJECTION MODEL** |
| **RQD increases e.g. 30 to 50%**<br>**Jn reduces e.g. 9 to 6**<br>**Jr increases e.g. 1 to 2**<br>**(due to sealing of most of set #1)**<br>**Ja reduces e.g. 2 to 1**<br>**(due to sealing of most of set #1)**<br>**Jw increases e.g. 0.5 to 1**<br>**SRF unchanged e.g.1.0 to 1.0** | **RQD increases e.g. 30 to 70%**<br>**Jn reduces e.g. 12 to 4**<br>**Jr increases e.g. 1.5 to 2**<br>**(due to sealing of most of set #1)**<br>**Ja reduces e.g. 4 to 1**<br>**(due to sealing of most of set #1)**<br>**Jw increases e.g. 0.66 to 1**<br>**SRF improves e.g. 2.5 to 1.0** |
| **WET CONDITIONS**<br>***Before pre-grouting***<br>***Q = 30/9 x 1/2 x 0.5/1 = 0.8*** | **WET CONDITIONS**<br>***Before pre-grouting***<br>**Q = 30/12 x 1.5/4 x 0.66/2.5 = 0.2** |
| *Vp ≈ 3.4 km/s*<br>$E_{mass}$ *≈ 9.3 GPa*<br>*K ≈ 1.3 x* $10^{-7}$ m/s<br>**e.g. for a 10 m tunnel: B 1.6 m c/c, S(fr) 10 cm** | *Vp ≈ 2.8 km/s*<br>$E_{mass}$ *≈ 5.8 GPa*<br>*K ≈ 5.0 x* $10^{-7}$ m/s<br>**e.g. for a 10 m tunnel: B 1.4 m c/c, S(fr) 13 cm** |
| **DRY CONDITIONS**<br>***After pre-grouting***<br>**Q = 50/6 x 2/1 x 1/1 = 17** | **DRY CONDITIONS**<br>***After pre-grouting***<br>**Q = 70/4 x 2/1 x 1/1 = 35** |
| ***Vp ≈ 4.7 km/s***<br>$E_{mass}$ ***≈ 25.7 GPa***<br>***K ≈ 5.9 x*** $10^{-9}$ ***m/s***<br>**e.g. for a 10 m tunnel: B 2.4 m c/c**<br>**(Today's conservatism may also demand a single layer of S(fr) due to the demand for lower ESR in the case of transport tunnels).** | ***Vp ≈ 5.0 km/s***<br>$E_{mass}$ ***≈ 32.7 GPa***<br>***K ≈ 2.9 x*** $10^{-9}$ ***m/s***<br>**e.g. for a 10 m tunnel: sb (spot bolts)**<br>**(Today's conservatism may also demand a single layer of S(fr) due to the demand for lower ESR in the case of transport tunnels).** |

RQD, and the *effective* Jn. There may also be transfer of lower Jr/Ja ratios to the remaining *uninjected* (probably tightest) joint sets, resulting in higher *effective* Jr/Ja ratios, and therefore to even higher *effective* post-injection Q-values.

In Barton (2002) there is documentation of the measured rotation of all principal permeability tensors (even) as a result of cement injection at a dam site. This was measured using 3D (multi-borehole) hydro-tomography by Quadros and Correa Filho (1995). So we know that joint sets can become sealed even at low pressures (max. 2 MPa) with non-ideal Portland cement and bentonite. With today's optimized grouting materials and the last 20 years of high pressure (5 to 10 MPa) pre-injection, as often practiced in Norway, it is perhaps time to take credit for the benefits of pre-injection, as already suggested by some tunnel contractors in Norway, who experienced first-hand the benefits of the improved conditions.

## Further Q-system applications – permeability may be related to 'Q-values'

An interesting and pre-injection related 'property' of the Q-value, clearly a result only possible with the big numerical range of Q, is that there is *some evidence* of an inverse relation between Q and the Lugeon value. This is strictly for the case of *clay-free rock masses*. Some theoretical justification is given in Barton (2006) (Chapter 9), based on the interpretation of a Lugeon test (with its 1 MPa over-pressure) as a slightly deforming test. A double Boussinesq 'foundation load' formulation is utilized, plus the cubic law relating flow rates to the cube of aperture, when apertures are large enough ( i.e. > 0.5mm). For details see Barton (2013).

Table 6 shows what to expect in approximate terms in (mostly clay-free) rock masses. Strong deviation from the simple scheme of values tabulated, in one direction or the other, would suggest the need to expect clay-filled discontinuities, or weak deformable rock like phyllite, or de-stressed rock, causing lower or higher permeability respectively, despite lower Q-values.

*Table 6 Ball-park estimation of permeability, when clay is absent. Barton (2006).There are valid theoretical arguments linking Lugeon and $Q_c$, because of deformability effects. $Q_c$ (= Q x $\sigma_c$) for the shale (Figure 28) might have increased due to pre-injection from 1 to an equivalent 100, with corresponding property improvements as a result: for example 0.01 Lugeon, and maybe also $V_P$ = 5.5 km/s.*

| $Q_c$ | 0.1 | 1 | 10 | 100 |
|---|---|---|---|---|
| Lugeon | 10 | 1 | 0.1 | 0.01 |
| K (m/s) | $10^{-6}$ | $10^{-7}$ | $10^{-8}$ | $10^{-9}$ |
| $V_P$ (km/s) | 2.5 | 3.5 | 4.5 | 5.5 |


*Figure 28 A successfully pre-injected tunnel (a completed section of the Bærum rail tunnel) which demonstrates a '99.999%' dry (non-humid) shotcrete.*

The obvious 'over-simplification' of the above inter-related parameters, in particular the inclusion of the inherently complicated *stress and depth dependent permeability* has resulted in the development of a more general '$Q_{H2O}$' model for estimating permeability. This has an empirically-developed depth dependence, and Jr/Ja is reversed to a more logical *Ja/Jr*. It is described in Barton (2013a).

## Further Q-system applications – Q in $Q_{TBM}$ prognosis

It is appropriate to end this illustrated guide to using Q, by giving a brief glimpse of Q when applied to TBM tunneling prognosis. In essence, the six Q parameters were added-to some fifteen years ago, in order to include TBM machine-rock interaction parameters, including the all-important comparison of rock mass strength (SIGMA) with the average cutter force F. Stage-by-stage development of the $Q_{TBM}$ prognosis model was described in Barton (2000).

On occasion and counter-intuitively, penetration rate (PR) can reduce despite increased cutter thrust. Remarkably, this seems to be an 'unknown' result for many working with TBM prognosis and performance. Nevertheless it is a documented result (Barton, 2000). It is caused by a rock/rock mass that has a sufficiently high strength such that it resists the effect of increased cutter thrust, and the penetration rate reduces. It is therefore most important to have a prognosis method in which cutter thrust is compared with an estimate of rock mass strength, and a prognosis result that can therefore match reality, i.e. reduced PR even with increased thrust when the rock is too strong and massive (high Q, high UCS).

The estimate of SIGMA is firmly Q-based, more specifically $Q_c$-based, in other words involving UCS. Using the $Q_{TBM}$ prognosis concerning PR, accuracy over a range of F=32 tons (high-powered TBM) down to F= 8 tons (blind-hole drilling) has been verified.

$$\text{SIGMA} = 5\gamma Q_c^{1/3} \tag{8}$$

where γ = rock density (gm/cm$^3$) and the units of SIGMA are MPa (range ≈ 1 to 100 MPa).

Another important aspect of TBM prognosis is to log RQD in the *tunneling direction*. This is especially important for TBM because steeply-dipping closely spaced jointing is easy to penetrate by (horizontal) TBM, but would show a confusingly high RQD in a vertical hole. Conversely, sub-horizontal jointing (or bedding) requires more rock-breaking energy, slowing PR, yet would exhibit a lower RQD if sampled with a vertical hole. ($RQD_o$ obtained from logging hundreds of rock cuttings for an imminent TBM tunnel near Oslo is shown in Fig. 31).

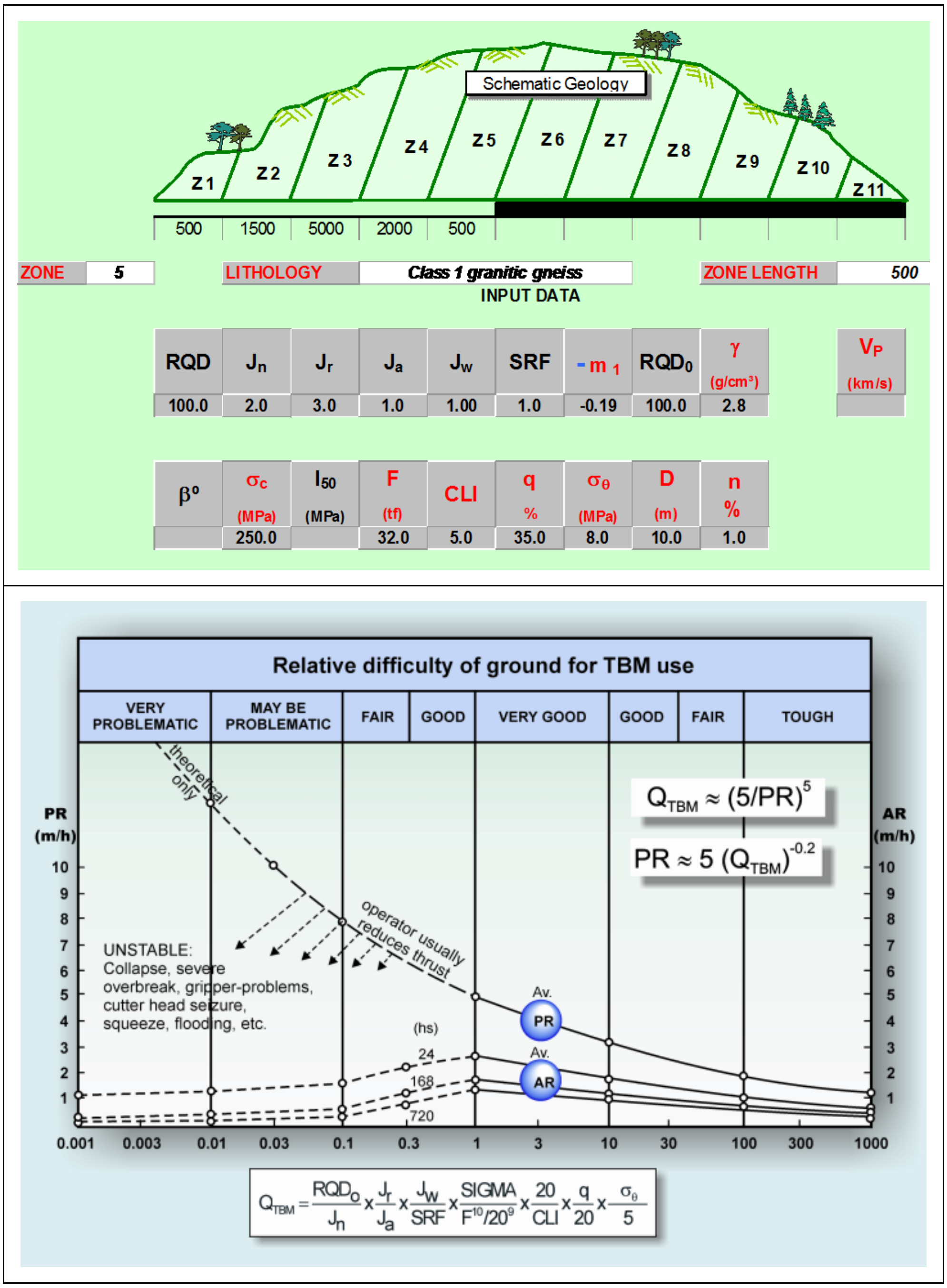


*Figure 29 Top: An example of the $Q_{TBM}$ prognosis model input data 'keyboard', which is entered with appropriate Q-parameter numbers for each zone modelled, whether 500m of massive granite (slow progress predicted as in this illustrated case) or a major fault zone (also slow progress or almost stoppage, due to reduced thrust and delays for support). Note that $m_1$ in the top row of the input data screen is the deceleration gradient which is strongly linked to the (regular) Q-value when the rock mass / tunneling quality is very poor (0.1 – 0.001: see red curved-line trends in Figure 30a). Bottom: The extended list of parameters given on the right-side of the six Q-parameters (with tunneling-oriented $RQD_0$), includes comparison of cutter force F (normalized by 20 tons) with an estimate of the rock mass strength SIGMA = $5\gamma Q_c^{1/3}$ MPa, where γ= density. The NTH/NTNU cutter life index term CLI, and the quartz content (q) are also used in a normalized format in the $Q_{TBM}$ model. The last $Q_{TBM}$ term is a tunnel depth correction, with the biaxial stress on the tunnel face ($\sigma_\theta$) assumed to be ≈ 5 MPa for each 100m of rock cover (so at 100m depth there is no influence). See Barton (2000 and 2013b) for $Q_{TBM}$ prognosis details.*

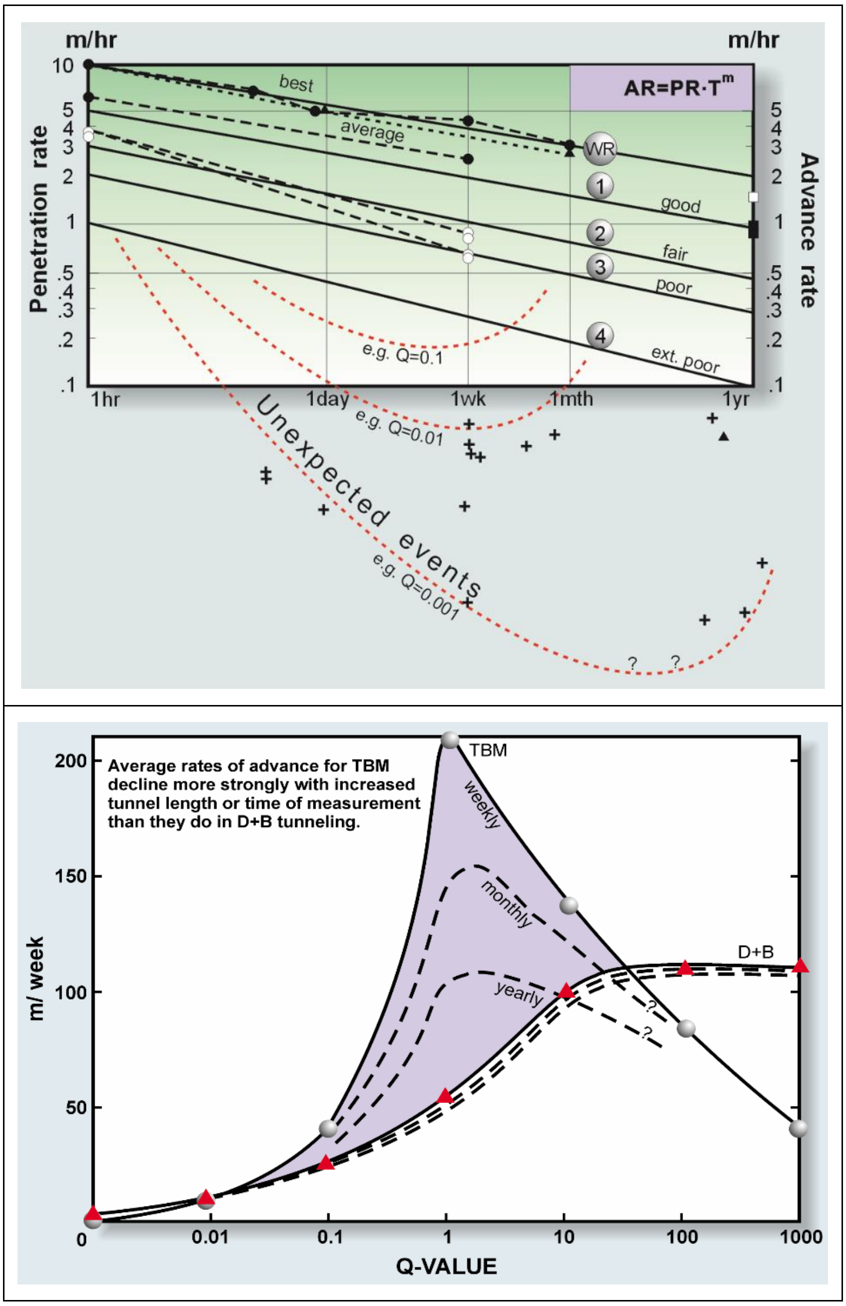


*Figure 30 Top: An analysis of 145 cases representing 1000 km of TBM tunnels, shows typical deceleration-with-time trends (see gradient –m) for mostly open-gripper case records. In fact double-shield case records follow similar trends, although the expected extra efficiency can reduce the deceleration gradients in some cases. Robbins numerous world records show similar deceleration with time period. EPB projects with picks and cutters follow similar but lower performance trends (Barton, 2013b).The 'unexpected events' – like stoppages in fault zones – are strongly related to low Q-values, so low Q-values usually mean steep negative (-m) deceleration gradients. (Note: utilization U = $T^{-m}$, where T is hours: i.e. utilization is time dependent, and therefore different advance rate AR curves are given in Figure 29b for 24 hours, 168 hours and 720 hours: 1 day, 1 week, 1 month). Bottom: An exercise comparing drill-and-blast (based on Norwegian cycle times) with a moderate TBM performance, which shows fast weekly averages, a bit slower monthly averages, and a one year performance that needs central $Q_{TBM}$ -values and central Q-values, if the TBM is to remain faster than drill-and-blast. Due to the normalization process, Q and $Q_{TBM}$ can have similar magnitudes, though may differ a lot when there is high or low cutter thrust.*

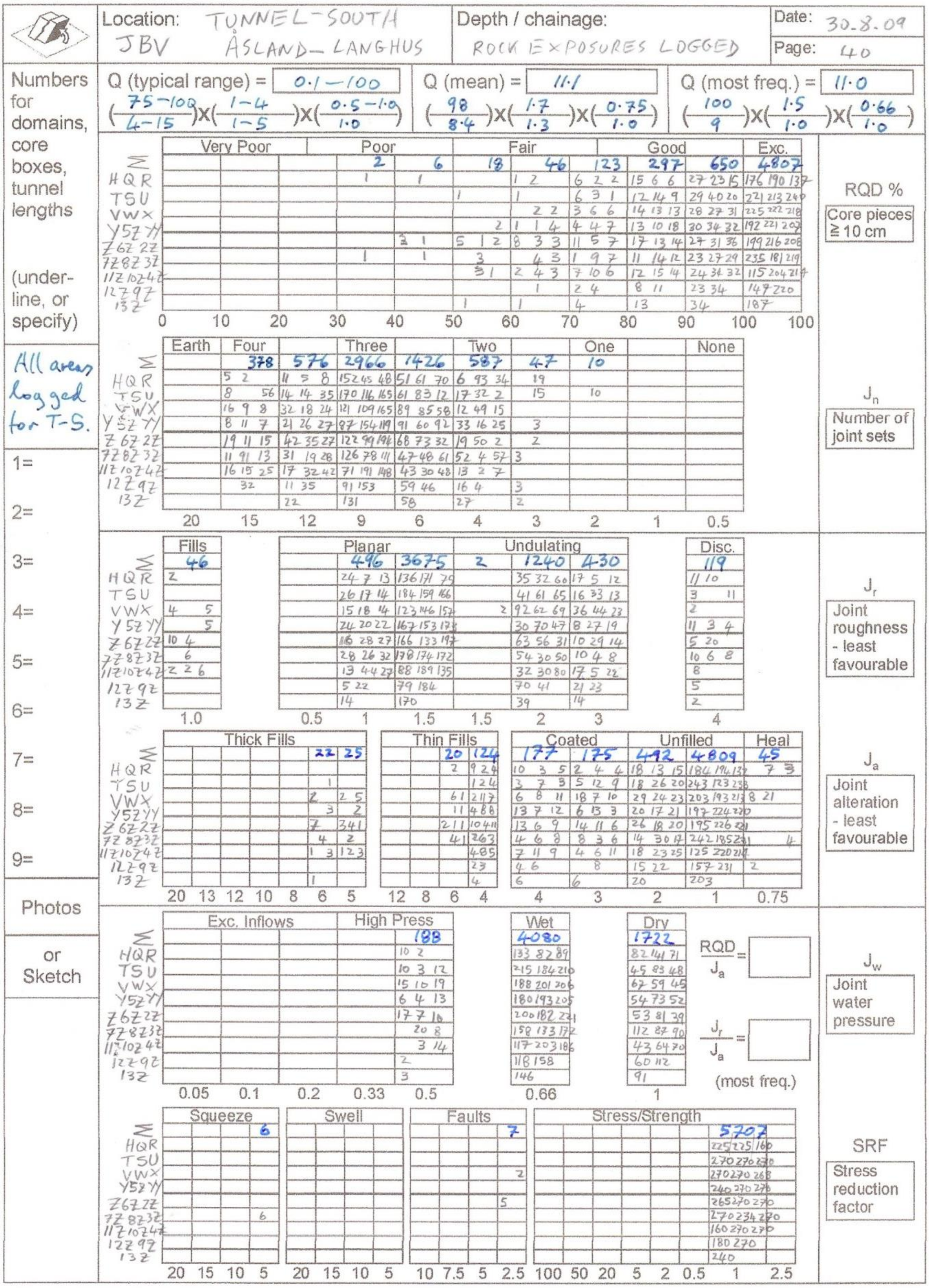


*Figure 31 An example of Q-parameter data collection from some 200 rock cuttings in the neighbourhood of a planned TBM tunnel (Oslo-Ski, southern tunnel of 8 km length). Five rock classes were identified, plus three more (not shown) as a result of weakness-zone core logging and seismic refraction P-wave velocity analysis. Barton and Gammelsæter (2010).*

Note that the (over-subscribed) letters of the alphabet (H, R, T, U, W, X, Z, 3Z, 8Z etc) written on the left of the field-logging sheet each refer to a specific rock cutting along which numerous (usually nine sets) of Q-parameters were logged. Five opinions of the most representative Q-parameter ratings were given for each 5m of cutting. More than 5,700 individual ratings are shown. In the case of Q-logging for TBM the Jr and Ja character of all the principal joint sets are recorded, as all may affect cutter penetration. The tunneling-oriented $RQD_o$ will already have reflected the most influential set for penetration (or lack of penetration), and this will likely dominate the Jr/Ja logging result. When logging Q for stability and tunnel support purposes, only the adversely oriented Jr/Ja statistics are utilized to calculate Q, as in the standard instructions referred to earlier in this illustrated Q-guide.

| Q - VALUES: | (RQD | / | Jn) | * | (Jr | / | Ja) | * | (Jw | / | SRF) | = | Q |
|---|---|---|---|---|---|---|---|---|---|---|---|---|---|
| Q (typical min)= | 75 | / | 15.0 | * | 1.0 | / | 5.0 | * | 0.50 | / | 1.0 | = | **0.500** |
| Q (typical max)= | 100 | / | 4.0 | * | 4.0 | / | 1.0 | * | 1.00 | / | 1.0 | = | **100.0** |
| Q (mean value)= | 98 | / | 8.4 | * | 1.7 | / | 1.3 | * | 0.75 | / | 1.0 | = | **11.07** |
| Q (most frequent)= | 100 | / | 9.0 | * | 1.5 | / | 1.0 | * | 0.66 | / | 1.0 | = | **11.00** |

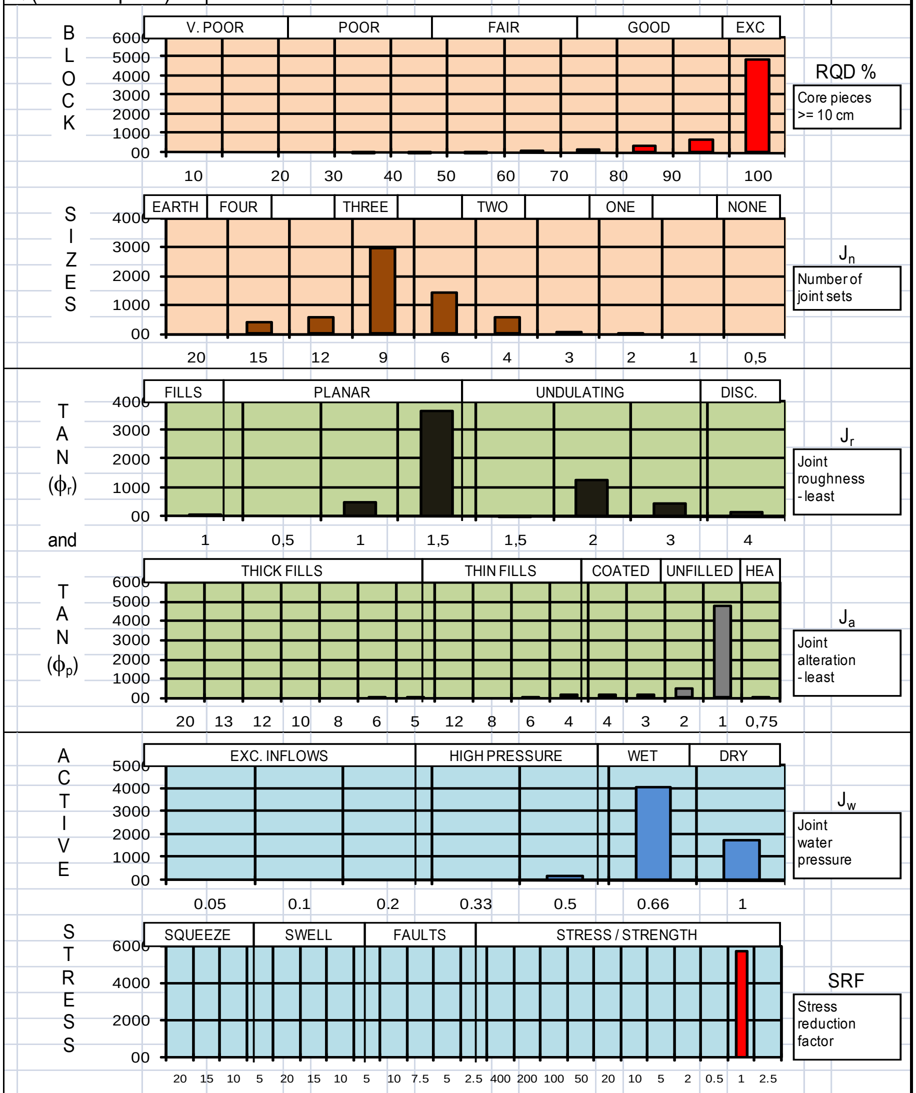


| | | | |
|---|---|---|---|
| **JBV OSLO-SKI** | Rev. | Report No. NB&A #1 | Figure No. 10 |
| Q-histogram based on compilation of all rock-exposure | Borehole No. : Rock slopes | Drawn by NB&A | Date 31.8.09 |
| logging for TUNNEL-SOUTH, therefore excluding core | Depth zone (m) near-surface | Checked nrb | |
| and weakness zones. | | Approved | |

*Figure 32  The same Q-parameter statistics (Figure 31) plotted with an EXCEL program.*

## Conclusions

1. The Q-value representing rock mass quality or lack of quality, and the Q-system linking Q to recommended single-shell permanent reinforcement and support measures (B + Sfr) has proved its value during its 40 years existence. It has been widely adopted both in Norway and in many other countries, as one of the standard empirical tools of rock mass characterization, and as a method for assisting in tunnel and cavern design in rock engineering.

2. The tunnel and cavern reinforcement and support measures were originally based on systematic bolting and mesh-reinforced shotcrete, when the Q-system was first developed in 1974. The development of wet process, robotically applied steel-fiber reinforced shotcrete saw first application in Norway in a hydropower cavern in 1979, and in Holmestrand road tunnel in 1981. The development of multi-layer corrosion protected (CT) bolts followed.

3. The Q-system support recommendations were updated in 1993 to reflect the widespread use of B+S(fr) as *single-shell permanent* support. There are about 1250 case records behind the method since 1993, and a further 800 cases since 2002. There are of course tens or hundreds of thousands of practical applications, the number depending on whether referring to individuals or groups of engineering geologists who apply Q on a 'daily' basis in numerous countries.

4. Besides its widespread use in civil engineering, the mining industry in all the principal mining countries (USA, Canada, Brazil, Peru, Chile, Australia etc.) make active use of the Q-system for support and reinforcement of 'permanent' mine roadways, and also make extensive use of the first four Q-parameters (RQD, Jn, Jr and Ja) together with stress/strength, stope dimensions, and structural orientation, when differentiating stable, transitional, or caving ground, meaning that the stopes are in need of temporary cable reinforcement. However, in civil engineering we recommend and need all six Q-parameters. The lack of a faulting term for mining stopes due to a consulting company's unilateral removal of SRF, and the lack of a Jw term for wet mines are potential weaknesses of the truncated Q' term.

5. The Q-value and its modified form $Q_c$, obtained by normalizing with UCS/100, has many potential uses in rock engineering. It can be correlated to the seismic P-wave velocity $V_P$ (km/s), the (static) deformation modulus M or $E_{mass}$ (GPa), the vertical and horizontal deformation, and has been linked tentatively with the Lugeon value of clay-free rock masses. In modified $Q_{H2O}$ form, depth-dependent permeability in the case of clay-bearing or deformable rock seems also to be predictable in approximate terms.

6. In the last 15 years the Q-value has been incorporated in a more comprehensive parameter called $Q_{TBM}$. This has additional machine-rock interaction parameters, and is used as a basis for TBM prognosis. On the basis of numerous (1000 km) of data linking TBM deceleration over time (also seen in world records), the Q-value in the case of poor rock conditions (Q<1) can be shown to explain delays and even stand-stills in fault zones. The gradient of deceleration relates strongly to Q-values.

## References


Austrian Society for Geomechanics (2010). NATM: The Austrian Practice of Conventional Tunnelling.

Barton, N., Lien, R. & Lunde, J. (1974). Engineering classification of rock masses for the design of tunnel support. *Rock Mechanics*. 6: 4: 189-236.

Barton, N. (1976). Unsupported underground openings. Rock Mechanics Discussion Meeting, Befo, Swedish Rock Mechanics Research Foundation, Stockholm, 61-94.

Barton, N., Grimstad, E., Aas, G., Opsahl, O.A., Bakken, A., Pedersen, L. & Johansen, E.D. (1992). Norwegian Method of Tunnelling. WT Focus on Norway, World Tunnelling, June/August 1992.

Barton, N. & Grimstad, E. (1994). The Q-system following twenty years of application in NMT support selection. *43rd Geomechanic Colloquy, Salzburg. Felsbau,* 6/94, 428-436.

Barton, N. (1994). A Q-system case record of cavern design in faulted rock. *5th Int. Rock Mechanics and Rock Engineering Conf., Tunnelling in difficult conditions,* Torino, Italy, 16.1-16.14.

Barton, N., By, T.L., Chryssanthakis, P., Tunbridge, L., Kristiansen, J., Løset, F., Bhasin, R.K., Westerdahl, H. & Vik, G. (1994). Predicted and measured performance of the 62m span Norwegian Olympic Ice Hockey Cavern at Gjøvik. *Int. J. Rock Mech, Min. Sci. & Geomech. Abstr.* 31:6: 617-641. Pergamon.

Barton, N. (1995). The influence of joint properties in modelling jointed rock masses. Keynote Lecture, *8th ISRM Congress*, Tokyo, 3: 1023-1032, Balkema, Rotterdam.

Barton, N. (1996). Investigation, design and support of major road tunnels in jointed rock using NMT principles. Keynote Lecture, IX Australian Tunnelling Conf. Sydney, 145-159.

Barton, N. (2000). *TBM tunnelling in jointed and faulted rock.* 173p. Balkema, Rotterdam.

Barton, N., Buen, B. & Roald, S. (2001). Strengthening the case for grouting Tunnels & Tunnelling International, Dec. 2001: 34-36, and Jan. 2002: 37-39.

Barton, N. (2002). Some new Q-value correlations to assist in site characterization and tunnel design. *Int. J. Rock Mech. & Min. Sci.* Vol. 39/2:185-216.

Barton, N. (2006). *Rock Quality, Seismic Velocity, Attenuation and Anisotropy*. Taylor & Francis, UK & Netherlands, 729 p.

Barton, N. & B. Gammelsæter (2010). Application of the Q-system and $Q_{TBM}$ prognosis to predict TBM tunnelling potential for the planned Oslo-Ski rail tunnels. *Nordic Rock Mechanics Conf*., Kongsberg, Norway.

Barton, N. (2011). From empiricism, through theory, to problem solving in rock engineering. ISRM Cong., Beijing. 6th Müller Lecture. Proceedings, Taylor & Francis, Vol. 1, Qian & Zhou (eds), 3-14.

Barton, N. (2012 a). Defining NMT as part of the NATM SCL debate. *TunnelTalk*, Ed. Shani Wallace. Sept. 2012, 4 p.

Barton, N. (2012 b). Assessing Pre-Injection in Tunnelling. Tunnelling Journal, Dec.2011/Jan. 2012, pp. 44-50.

Barton, N. (2013 a). Integrated empirical methods for the design of tunnels, shafts and caverns in rock, based on the Q-system. 3rd Int. Symp. on *Tunnels and Shafts in Soil and Rock*, SMIG/Amitos, 17p. Nov. 2013, Mexico City.

Barton, N. (2013 b). TBM prognoses for open-gripper and double-shield machines: challenges and solutions for weakness zones and water. FJELLSPRENGNINGSTEKNIKK – BERGMEKANIKK – GEOTEKNIKK, Oslo, 21.1-21.17.

Barton, N. (2014). Lessons learned using empirical methods applied in mining. Keynote lecture. 1st. Int. Conf. on Applied Empirical Methods in Mining. Lima, Peru, 24p.

Barton, N. and Grimstad, E. (2014). 40 years of Q-system lessons. Tunnelling Journal.

Bieniawski, Z.T. (1989). Engineering rock mass classifications: A complete manual for engineers and geologists in mining, civil and petroleum engineering. 251 p. J. Wiley.

Grimstad, E. & Barton, N. (1993). Updating of the Q-System for NMT. *Proc. of Int. Symp. on Sprayed Concrete - Modern Use of Wet Mix Sprayed Concrete for Underground Support,*

Fagernes, 1993, (Eds Kompen, Opsahl and Berg. Norwegian Concrete Association, Oslo, 46-66.
Grimstad, E. (1996), Stability in hard rock affected by high stress and supported by sprayed concrete and rock bolts. *Proc., 2nd Int. Symp. On Sprayed Concrete, Modern use of wet mix sprayed concrete for underground support.* Gol, Norway.
Grimstad, E., K. Kankes, R. Bhasin, A. W. Magnussen and A . Kaynia (2002). Rock Mass Q used in designing Reinforced Ribs of Sprayed Concrete and Energy Absorption" *4th Int. Symp. on Sprayed Concrete*, Davos, Switzerland.
Grimstad, E., K.Kankes, R. Bhasin, A. W. Magnussen and A.Kaynia (2003).Updating the Q-system for Designing Reinforced Ribs of Sprayed Concrete and General Support. Proceedings, *Underground Construction,* London.
Grimstad, E. (2007). The Norwegian method of tunnelling – a challenge for support design. *XIV European Conference on Soil Machanics and Geotechnical Engineering.* Madrid.
Grimstad, E., Tunbridge, L., Bhasin, R., and Aarset, A. (2008). Measurements of Forces in Reinforced Ribs of Sprayed Concrete. *5th. Int. Conf. on Sprayed Concrete*. Lillehammer, Norway.
Kristiansen, J. and Hansen, S.E. (1993). Cavern Stadium – displacement measurements. *Final Report on the Research Project for the Rock Cavern Stadium,* SINTEF-NGI-Østlandsforskning, Norway.
Løset, F. and Bhasin, R. (1992). Engineering geology – Gjøvik Ice Hockey Cavern. *Research Project: 'Publikumshall I Berg',* SINTEF-NGI-Østlandsforskning, Norway.
Quadros, E. F. & Correa Filho, D. (1995). Grouting efficiency using directional (3-D) hydraulic tests in Pirapora Dam, Brazil. Proc. 8th ISRM congress, Tokyo. Fujii, ed., 823-826.
Sjøgren, B., Øfsthus, A. & Sandberg, J. (1979). Seismic classification of rock mass qualities. *Geophys. Prospect.,* 27: 409-442.
Ward, W.H., P. Todd and N.S.M.Berry. (1983). The Kielder Experimental Tunnel: Final Results. Geotechnique 33, 3, 275-291.
Vandevall, M. (1990). *Dramix - Tunnelling the World.* NV Bækert S.A, 1991 edition.

APPENDIX A1 – Q-parameter definitions and ratings for reference. The Q-logging sheet (following page) is an abbreviated form of these tables used when logging in the field (drill-core, rock exposures, or tunnel advances). See Appendix A4 for details of Jr/Ja, and Appendix A5, Tables A5.1 and A5.2 for specific high stress data related to the highest SRF values in the case of massive rock.

| | **1. Rock Quality Designation** | **RQD (%)** |
|---|---|---|
| A | Very poor | 0-25 |
| B | Poor | 25-50 |
| C | Fair | 50-75 |
| D | Good | 75-90 |
| E | Excellent | 90-100 |

*Notes: i) Where RQD is reported or measured as ≤ 10 (including 0), a nominal value of 10 is used to evaluate Q.*
*ii) RQD intervals of 5, i.e., 100, 95, 90, etc., are sufficiently accurate.*

| | **2. Joint set number** | **$J_n$** |
|---|---|---|
| A | Massive, no or few joints | 0.5-1 |
| B | One joint set | 2 |
| C | One joint set plus random joints | 3 |
| D | Two joint sets | 4 |
| E | Two joint sets plus random joints | 6 |
| F | Three joint sets | 9 |
| G | Three joint sets plus random joints | 12 |
| H | Four or more joint sets, random, heavily jointed, 'sugar-cube', etc. | 15 |
| J | Crushed rock, earthlike | 20 |

*Notes: i) For tunnel intersections, use $(3.0 \times J_n)$.*
*ii) For portals use $(2.0 \times J_n)$.*

| | **3. Joint roughness number** | **$J_r$** |
|---|---|---|
| | ***a) Rock-wall contact, and b) Rock-wall contact before 10 cm shear*** | |
| A | Discontinuous joints | 4 |
| B | Rough or irregular, undulating | 3 |
| C | Smooth, undulating | 2 |
| D | Slickensided, undulating | 1.5 |
| E | Rough or irregular, planar | 1.5 |
| F | Smooth, planar | 1.0 |
| G | Slickensided, planar | 0.5 |

*Notes: i) Descriptions refer to small-scale features and intermediate scale features, in that order.*

| | ***b) No rock-wall contact when sheared*** | |
|---|---|---|
| H | Zone containing clay minerals thick enough to prevent rock-wall contact. | 1.0 |
| J | Sandy, gravely or crushed zone thick enough to prevent rock-wall contact | 1.0 |

*Notes: ii) Add 1.0 if the mean spacing of the relevant joint set is greater than 3 m.*
*iii) $J_r$ = 0.5 can be used for planar, slickensided joints having lineations, provided the lineations are oriented for minimum strength.*
*iv) $J_r$ and $J_a$ classification is applied to the joint set or discontinuity that is least favourable for stability both from the point of view of orientation and shear resistance, $\tau$ (where $\tau \approx \sigma_n \tan^{-1}(J_r/J_a)$).*

Barton

| | **4. Joint alteration number** | **$\phi_r$ approx.** | **$J_a$** |
|---|---|---|---|
| | ***a) Rock-wall contact (no mineral fillings, only coatings)*** | | |
| A | Tightly healed, hard, non-softening, impermeable filling, i.e., quartz or epidote. | -- | 0.75 |
| B | Unaltered joint walls, surface staining only. | 25-35° | 1.0 |
| C | Slightly altered joint walls. Non-softening mineral coatings, sandy particles, clay-free disintegrated rock, etc. | 25-30° | 2.0 |
| D | Silty- or sandy-clay coatings, small clay fraction (non-softening). | 20-25° | 3.0 |
| E | Softening or low friction clay mineral coatings, i.e., kaolinite or mica. Also chlorite, talc, gypsum, graphite, etc., and small quantities of swelling clays. | 8-16° | 4.0 |
| | ***b) Rock-wall contact before 10 cm shear (thin mineral fillings).*** | | |
| F | Sandy particles, clay-free disintegrated rock, etc. | 25-30° | 4.0 |
| G | Strongly over-consolidated non-softening clay mineral fillings (continuous, but < 5 mm thickness). | 16-24° | 6.0 |
| H | Medium or low over-consolidation, softening, clay mineral fillings (continuous, but < 5 mm thickness). | 12-16° | 8.0 |
| J | Swelling-clay fillings, i.e., montmorillonite (continuous, but < 5 mm thickness). Value of $J_a$ depends on per cent of swelling clay-size particles, and access to water, etc. | 6-12° | 8-12 |
| | ***c) No rock-wall contact when sheared (thick mineral fillings)*** | | |
| KL M | Zones or bands of disintegrated or crushed rock and clay (see G, H, J for description of clay condition). | 6-24° | 6, 8, or 8-12 |
| N | Zones or bands of silty- or sandy-clay, small clay fraction (non-softening). | -- | 5.0 |
| OP R | Thick, continuous zones or bands of clay (see G, H, J for description of clay condition). | 6-24° | 10, 13, or 13-20 |

| | **5. Joint water reduction factor** | **approx. water pres. (kg/cm²)** | **$J_w$** |
|---|---|---|---|
| A | Dry excavations or minor inflow, i.e. < 1 litre/min locally. | < 1 | 1.0 |
| B | Medium inflow or pressure, i.e. < 5 litre/min locally, occasional outwash of joint fillings. | 1-2.5 | 0.66 |
| C | Large inflow or high pressure in competent rock with unfilled joints. | 2.5-10 | 0.5 |
| D | Large inflow or high pressure, considerable outwash of joint fillings. | 2.5-10 | 0.33 |
| E | Exceptionally high inflow or water pressure at blasting, decaying with time. | > 10 | 0.2-0.1 |
| F | Exceptionally high inflow or water pressure continuing without noticeable decay. | > 10 | 0.1-0.05 |

*Notes: i) Factors C to F are crude estimates. Increase $J_w$ if drainage measures installed.*
*ii) Special problems caused by ice formation are not considered.*
*iii) For general **characterization** of rock masses distant from excavation influences, the use of Jw = 1.0, 0.66, 0.5, 0.33 etc. as depth increases from say 0-5m, 5-25m, 25-250m to >250m is recommended, assuming that RQD /Jn is low enough (e.g. 0.5-25) for good hydraulic connectivity. This will help to adjust Q for some of the effective stress and water softening effects, in combination with appropriate **characterization** values of SRF. Correlations with depth-dependent static deformation modulus and seismic velocity will then follow the practice used when these were developed.*

| | **6. Stress Reduction Factor** | **SRF** |
|---|---|---|
| | ***a) Weakness zones intersecting excavation, which may cause loosening of rock mass when tunnel is excavated*** | |
| A | Multiple occurrences of weakness zones containing **clay** or chemically disintegrated rock, very loose surrounding rock (any depth). | 10 |
| B | Single weakness zones containing **clay** or chemically disintegrated rock (depth of excavation ≤ 50 m). | 5 |
| C | Single weakness zones containing **clay** or chemically disintegrated rock (depth of excavation > 50 m). | 2.5 |
| D | Multiple shear zones in competent rock (**clay-free**), loose surrounding rock (any depth). | 7.5 |
| E | Single shear zones in competent rock (**clay-free**), (depth of excavation ≤ 50 m). | 5.0 |
| F | Single shear zones in competent rock (**clay-free**), (depth of excavation > 50 m). | 2.5 |
| G | Loose, open joints, heavily jointed or 'sugar cube', etc. (any depth) | 5.0 |

*Notes: i) Reduce these values of SRF by 25-50% if the relevant shear zones only influence but do not intersect the excavation. This will also be relevant for **characterization**.*

| | ***b) Competent rock, rock stress problems*** | **$\sigma_c/\sigma_1$** | **$\sigma_\theta/\sigma_c$** | **SRF** |
|---|---|---|---|---|
| H | Low stress, near surface, open joints. | > 200 | < 0.01 | 2.5 |
| J | Medium stress, favourable stress condition. | 200-10 | 0.01-0.3 | 1 |
| K | High stress, very tight structure. Usually favourable to stability, may be unfavourable for wall stability. | 10-5 | 0.3-0.4 | 0.5-2 |
| L | Moderate slabbing after > 1 hour in **massive** rock. | 5-3 | 0.5-0.65 | 5-50 |
| M | Slabbing and rock burst after a few minutes in **massive** rock. | 3-2 | 0.65-1 | 50-200 |
| N | Heavy rock burst (strain-burst) and immediate dynamic deformations in **massive** rock. | < 2 | > 1 | 200-400 |

*Notes: ii) For strongly anisotropic virgin stress field (if measured): When $5 \le \sigma_1/\sigma_3 \le 10$, reduce $\sigma_c$ to $0.75\,\sigma_c$. When $\sigma_1/\sigma_3 > 10$, reduce $\sigma_c$ to $0.5\,\sigma_c$, where $\sigma_c$ = unconfined compression strength, $\sigma_1$ and $\sigma_3$ are the major and minor principal stresses, and $\sigma_\theta$ = maximum tangential stress (estimated from elastic theory).*
*iii) Few case records available where depth of crown below surface is less than span width. Suggest an SRF increase from 2.5 to 5 for such cases (see H).*
*iv) Cases L, M, and N are usually most relevant for support design of deep tunnel excavations in hard massive rock masses, with RQD /Jn ratios from about 50 to 200.*
*v) For general **characterization** of rock masses distant from excavation influences, the use of SRF = 5, 2.5, 1.0, and 0.5 is recommended as depth increases from say 0-5m, 5-25m, 25-250m to >250m. This will help to adjust Q for some of the effective stress effects, in combination with appropriate **characterization** values of Jw. Correlations with depth - dependent static deformation modulus and seismic velocity will then follow the practice used when these were developed.*

| | ***c) Squeezing rock: plastic flow of incompetent rock under the influence of high rock pressure*** | **$\sigma_\theta/\sigma_c$** | **SRF** |
|---|---|---|---|
| O | Mild squeezing rock pressure | 1-5 | 5-10 |
| P | Heavy squeezing rock pressure | > 5 | 10-20 |

*Notes: vi) Cases of squeezing rock may occur for depth $H > 350\,Q^{1/3}$ according to Singh 1993. Rock mass compression strength can be estimated from $SIGMA_{cm} \approx 5\,\gamma Q_c^{1/3}$ (MPa) when $\gamma$ = rock density in t/m³, and $Q_c = Q \times \sigma_c/100$, Barton, 2000 [29].*

| | ***d) Swelling rock: chemical swelling activity depending on presence of water*** | **SRF** |
|---|---|---|
| R | Mild swelling rock pressure | 5-10 |
| S | Heavy swelling rock pressure | 10-15 |

APPENDIX A2 – Empty Q-parameter logging sheet. Note (brief) descriptions and ratings above and below each space for recording number of observations. It is convenient to number each row (1 to 9 and result Σ) on the left side, in order to correctly locate (by row) the 5m of core, or 5 m of tunnel being logged e.g. 1= 76.1-81.1m, 2= 81.1-86.1m etc. One can then return to zones (domains, rock types, fault zones) and extract specific observations for separate analysis. Allow five observations per 5m observed (core, exposure, tunnel wall).

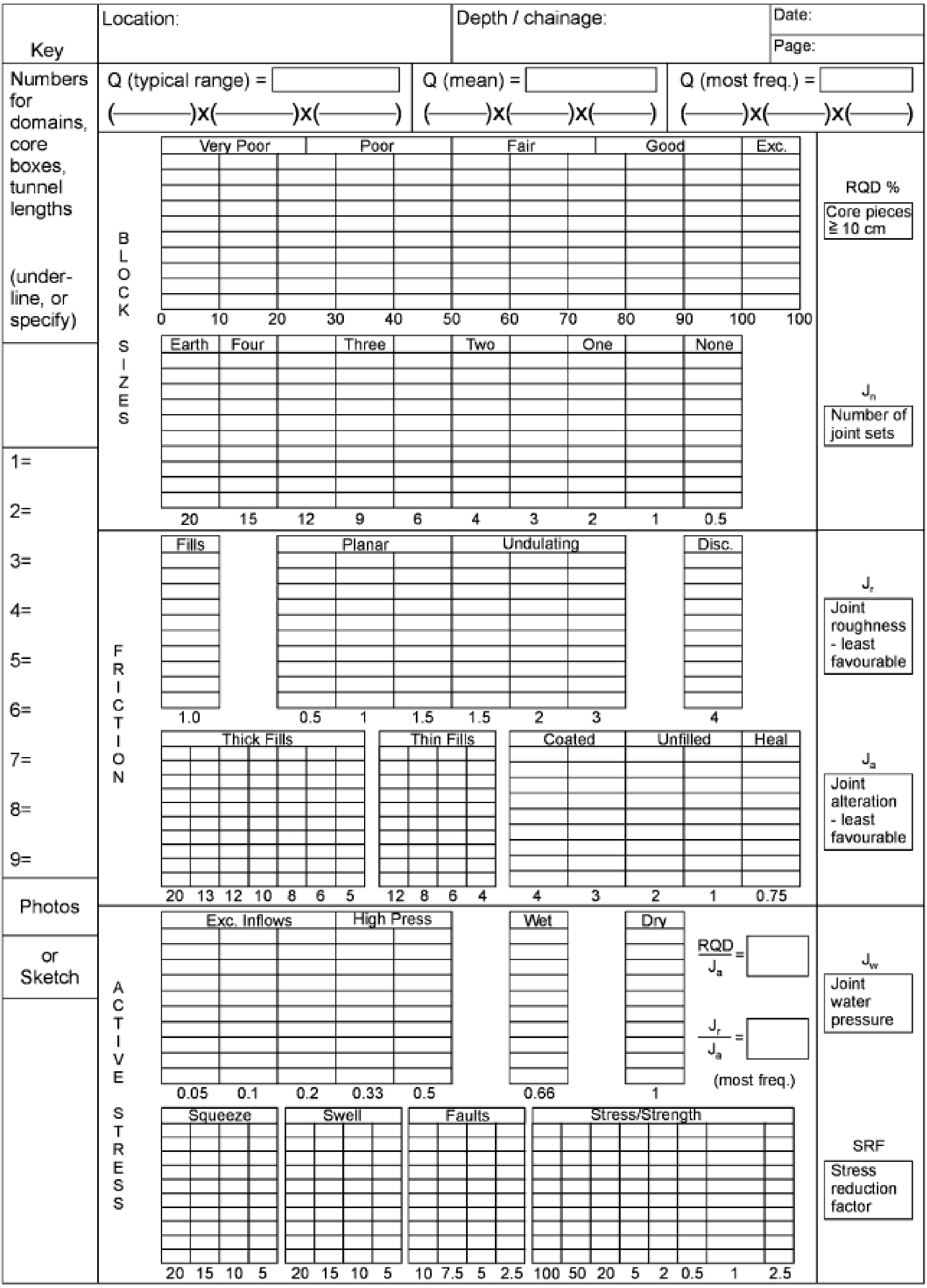

APPENDIX A3 – Completed logging sheet with EXCEL calculation of simple Q-statistics. Note weathered, heavily jointed, sheared and clay-bearing nature of this (ore-body) rock mass.

| Q - VALUES: | (RQD | / | Jn) | * | (Jr | / | Ja) | * | (Jw | / | SRF) | = | Q |
|---|---|---|---|---|---|---|---|---|---|---|---|---|---|
| Q (typical min)= | 10 | / | 15,0 | * | 1,0 | / | 6,0 | * | 0,66 | / | 2,5 | = | **0,029** |
| Q (typical max)= | 75 | / | 6,0 | * | 4,0 | / | 2,0 | * | 1,00 | / | 1,0 | = | **25,0** |
| Q (mean value)= | 38 | / | 12,8 | * | 2,4 | / | 3,9 | * | 0,94 | / | 1,3 | = | **1,29** |
| Q (most frequent)= | 10 | / | 15,0 | * | 3,0 | / | 2,0 | * | 1,00 | / | 1,0 | = | **1,00** |

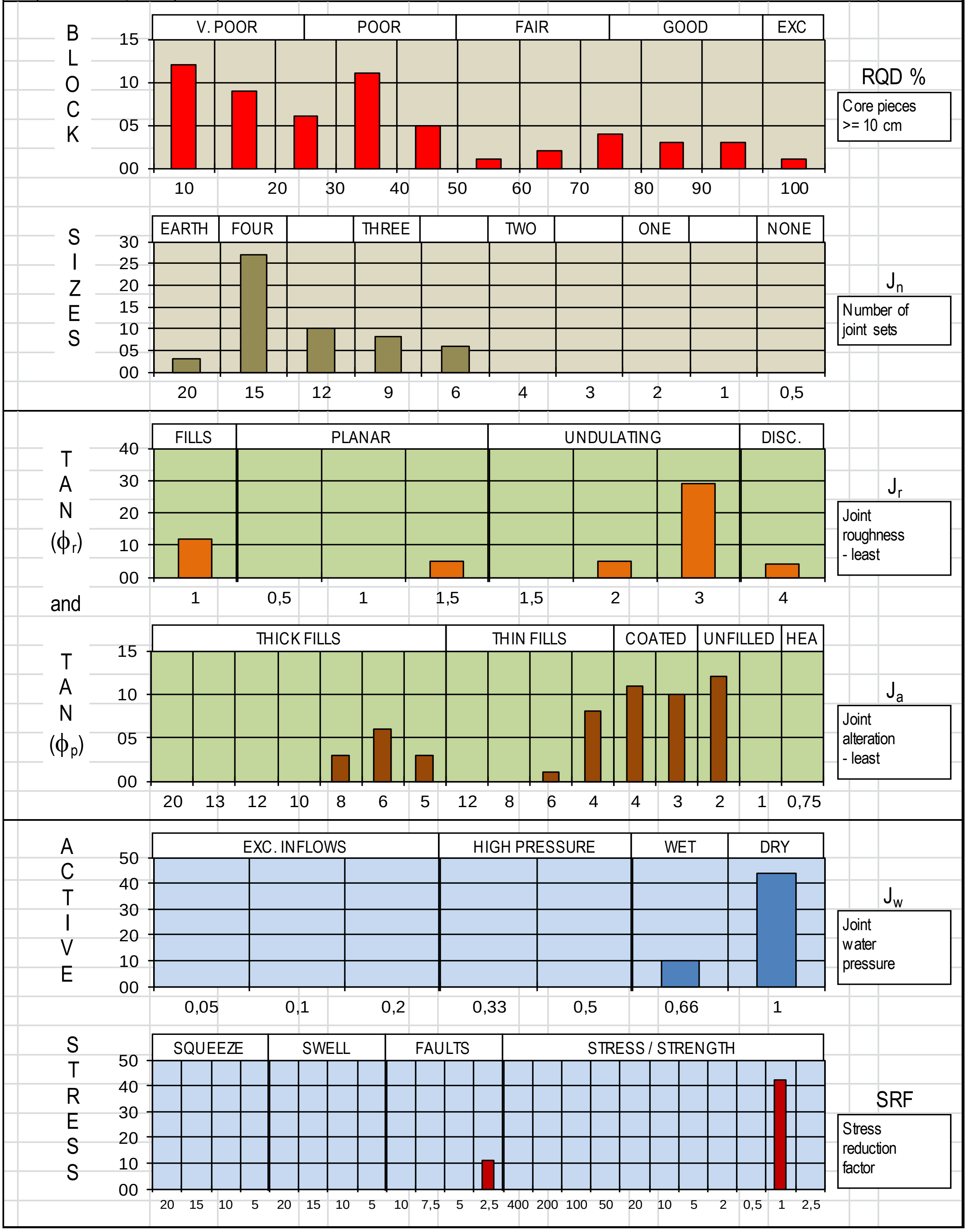

APPENDIX A4 – An important feature of the Q-value calculation is the ratio Jr/Ja representing the frictional strength, and closely resembling the inter-block friction coefficient. Therefore $\tan^{-1}$ (Jr/Ja) gives a rough indication of the friction angle, with a 'dilational' component seemingly added in the top-left friction angles, and a 'contractile' component subtracted in the bottom-right friction angles. Note the three contact categories, and the symbolic shear strength-displacement diagrams for each case. The above frictional reality was an accidental development of Barton et al. (1974), which was discovered after all Q-parameter ratings were finalized. In fact $Q_c$ resembles 'c' x 'tan φ' (Barton, 2012).

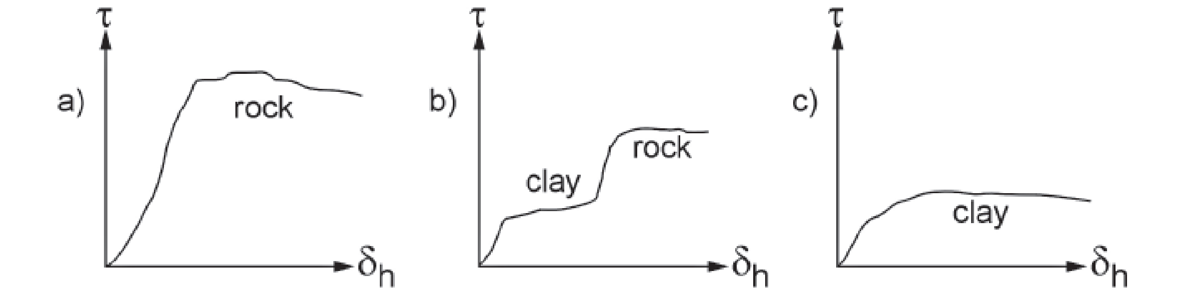


(a) Rock wall contact

| | Jr | Ja/Jr = 0.75 | 1.0 | 2 | 3 | 4 |
|---|---|---|---|---|---|---|
| | | (thin coatings) tan⁻¹(Jr/Ja)° | | | | |
| A. Discontinuous joints | 4 | 79° | 76° | 63° | 53° | 45° |
| B. Rough, undulating | 3 | 76° | 72° | 56° | 45° | 37° |
| C. Smooth, undulating | 2 | 69° | 63° | 45° | 34° | 27° |
| D. Slickensided, undulating | 1.5 | 63° | 56° | 37° | 27° | 21° |
| E. Rough, planar | 1.5 | 63° | 56° | 37° | 27° | 21° |
| F. Smooth, planar | 1.0 | 53° | 45° | 27° | 18° | 14° |
| G. Slickensided, planar | 0.5 | 34° | 27° | 14° | 9.5° | 7.1° |

(b) Rock wall contact when sheared

| | Jr | Ja/Jr = 4 | 6 | 8 | 12 |
|---|---|---|---|---|---|
| | | (thin fillings) tan⁻¹(Jr/Ja)° | | | |
| A. Discontinuous joints | 4 | 45° | 34° | 27° | 18° |
| B. Rough, undulating | 3 | 37° | 27° | 21° | 14° |
| C. Smooth, undulating | 2 | 27° | 18° | 14° | 9.5° |
| D. Slickensided, undulating | 1.5 | 21° | 14° | 11° | 7.1° |
| E. Rough, planar | 1.5 | 21° | 14° | 11° | 7.1° |
| F. Smooth, planar | 1.0 | 14° | 9.5° | 7.1° | 4.7° |
| G. Slickensided, planar | 0.5 | 7° | 4.7° | 3.6° | 2.4° |

(c) No rock wall contact when sheared

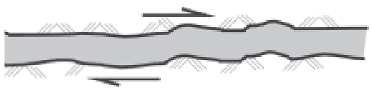

| | Jr | Ja/Jr = 5 | 6 | 8 | 12 | 13 | 16 | 20 |
|---|---|---|---|---|---|---|---|---|
| | | (thick fillings) tan⁻¹(Jr/Ja)° | | | | | | |
| Nominal roughness of discontinuity rock walls | 1.0 | 11.3° | 9.5° | 7.1° | 4.8° | 4.4° | 3.6° | 2.9° |

APPENDIX A5 – Observations of high stresses in deep tunnels (Grimstad, 1996).

Table A5.1 The table shows overburden, measured and estimated compressive strengths and principal stresses, $\sigma_c$, $\sigma_1$, $\sigma_3$, calculated tangential stress $\sigma_\theta$, and the relations $\sigma_c/\sigma_1$ and $\sigma_\theta/\sigma_c$ at some Norwegian road tunnels and at two hydropower schemes in Chile and China. Grimstad, 1996. As with mining and nuclear waste project data, when the ratio $\sigma_\theta/\sigma_c \geq 0.4$ (approx.) stress slabbing begins, requiring SRF ≥ 5 (see Appendix A1, Table 6b and Table A5.2 below).

| **Name** | **Rock type** | **Overburden (m)** | **$\sigma_1$ MPa** | **$\sigma_3$ MPa** | **$\sigma_c$ MPa** | **Max.$\sigma_\theta$ MPa** | **$\sigma_c/\sigma_1$** | **$\sigma_\theta/\sigma_c$** |
|---|---|---|---|---|---|---|---|---|
| Strynefjellet | Banded gneiss | 230-600** | 20.4 | 3.5 | 47-127 | 56 | 4.3 | 0.4-1.2 |
| Høyanger I | Granitic gneiss | 650-800** | 33.4 | 8.1 | 100-177 | 92 | 3.0-5.3 | 0.5-0.9 |
| Høyanger II | Banded gneiss | 900-1100** | 29 | 14 | 55-126 | 73 | 1.9-4.3 | 0.6-1.3 |
| Kobbskaret | Granite | 200-600* ** | 26 | 11.5 | 90 | 67 | 3.5 | 0.7 |
| Svartisen I | Granite | 700** | 21.4 | 12.1 | 181 | 52 | 8.4 | 0.3 |
| Svartisen II | Mica gneiss | 500 Δ | 10.9 | 8.1 | 27 | 25 | 2.5 | 0.9 |
| Tafjord | Gneiss, amphib. | 500-1200*Δ | 24.8 | 6.6 | 82-185 | 68 | 3.3-7.4 | 0.4-0.8 |
| Fjærland | Granitic gneiss | 600-1200** | 25.7 | 6.5 | 110 | 71 | 4.2 | 0.7 |
| Frudalen | Granitic gneiss | 900-1200**Δ | 30 ? | 20 ? | 70-150 | ca. 70 | 2.3-6.0 | 0.4-1.0 |
| Tosen | Silicate gneiss | 400-600** | 20 ? | 10 ? | 110-200 | ca. 50 | 5.5-10 | 0.3-0.5 |
| Fodnes | Gabbro, diorite | 650-1100*Δ | 30 ? | 15 ? | 100-150 | ca. 75 | 3.3-5.0 | 0.5-0.8 |
| Amla | Gabbro, diorite | 100-400** | 20 ? | 5-10 ? | 100-150 | ca. 50 | 5-7.5 | 0.3-0.5 |
| Lærdal | Banded gneiss | 800-1400** | 40 ? | 22 ? | 100-150 | ca.100 | 2.5-3.8 | 0.7-1.0 |
| Stetind | Granite | 300-500?*Δ | 9.3 | 3.8 | 90 | 24 | 10 | 0.3 |
| Pehuencha, Chile | Andesite | 400-1200 Δ | 35 ? | 15 ? | 100-150 | ca. 75 | 2.9-4.3 | 0.5-0.8 |
| Ertan, China | Gabbro, diorite | 300-400* ** | 40 ? | 15 ? | 105-160 | ca. 90 | 2.7-4.5 | 0.6-0.9 |

***Sub-horizontal major principal stress. * Valley side stress. Δ Sub-vertical stress. The compressive strength of the rock mass is often less than $\sigma_c$ because of jointing.*

*Table A5.2 Relation between uniaxial compressive strength $\sigma_c$ and major principal stress $\sigma_1$, and between tangential stress $\sigma_\theta$ and $\sigma_c$, with each compared to deformation duration time, and to estimated total deformation. Estimated SRF values are also given. Grimstad,1996.*

| **Name/place** | **$\sigma_c/\sigma_1$** | **$\sigma_\theta/\sigma_c$** | **SRF** | **Deformation time before observation** | **Type of damage** | **Estimated total deformation** |
|---|---|---|---|---|---|---|
| Strynefjellet | 4.3 | 0.4-1.2 | 5-200 | 16-21 years | SlR | 20-60 ?mm |
| Høyanger I | 3-5.3 | 0.5-0.9 | 5-150 | 4-8 years | SpR + DP | 10-40 ?mm |
| Høyanger II | 1.9- | 0.6-1.3 | 50-400 | 4-8 years | SpR + DP | 20-100 ?mm |
| Kobbskaret | 3.5 | 0.7 | 50 | 2-24 months | SpR | 20-50 ?mm |
| Svartisen II | 2.5 | 0.9 | 150 | 6-18 months | SpR | 30-50 ?mm |
| Tafjord | 3.3- | 0.4-0.8 | 5-100 | 2-3 years | SpR + $SlS_{fr}$ | 10-50 ?mm |
| Fjærland | 4.2 | 0.7 | 50 | 5-7 years | SpR | 10-40 ?mm |
| Frudalen | 2.3- | 0.4-1.0 | 5-200 | 1 - 25 weeks | $CrS_{fr}$ + SpR | 20-60 ?mm |
| Tosen | 5.5-10 | 0.3-0.5 | 2-5 | 2-12 months | SpR | 1-20 ?mm |
| Fodnes | 3.3- | 0.5-0.8 | 5-150 | 1-12 months | SpR+$CrS_{fr}$+ | 20-60 ?mm |
| Amla | 5-7,5 | 0.3-0.5 | 2-5 | 1 week-2 | SpR + $CrS_{fr}$ | 1-10 ?mm |
| Lærdalstunn. | 2,5- | 0,7-1,0 | 50-400 | 1-8 weeks | SpR+$CrS_{fr}$+ | 40-200 ?mm |
| Stetind | 4 | 0,7 | 50 - 100 | 4-5 years | $CrS_{fr}$ + $SlS_{fr}$ | 10-60 ?mm |
| Pehuenche, | 2.9- | 0.5-0.8 | 200-400❖ | 3-16 weeks | $SlS_{mr}$ + DP | 20-100 ?mm |
| Ertan, China | 2.7- | 0.6-0.9 | 50-200 | 1-24 months | $SlS_{fr,/mr/p}$ + | 20-160 mm |

❖ The compressive strength of the *rock mass* is less than $\sigma_c$ because of jointing

*Type of damage:* SpR = spalling in rock, SlR = slabbing in rock, $CrS_{fr}$ = cracks in steel fibre reinforced shotcrete, $CrS_{mr}$ = cracks in mesh reinforced shotcrete, $SlS_{fr}$ = slabbing in steel fibre reinforced shotcrete, $SlS_{mr}$ = slabbing in mesh reinforced shotcrete, $SlS_p$ = slabbing in plain shotcrete, TB = torn off rock bolts, PB = pulled out rock bolts, DP = deformed or torn off plates on rock bolts

APPENDIX A6 – Case records for shotcrete thickness and bolt spacing from some 800 cases collected by Grimstad, where the Q-system recommendations *were mostly not used* by the designers, which also resulted in occasional failures. Similar data for 1050 cases were given in Grimstad and Barton (1993). A German critic has suggested the scatter represents failure of the Q-system. An alternative explanation is that the multiple designers of these case records were lacking guidance, especially on bolt spacing.